STUDIES ON THE EFFECT OF SWIRL INTENSITY AND FUEL MIXTURES ON COMBUSTION AND FLAME CHARACTERISTICS OF SWIRL BURNER

(KAJIAN KE ATAS KESAN KEAMATAN PUSARAN DAN CAMPURAN BAHAN API TERHADAP PEMBAKARAN DAN CIRI NYALAAN PEMBAKAR PUSARAN)

DR. MAZLAN ABDUL WAHID
ASSOC. PROF. DR NAZRI M. JAAFAR
PROF.DR.IR. FARID NASIR ANI

RESEARCH VOTE NUM:
75181

Jabatan Termo-Bendalir
Fakulti Kejuruteraan Mekanikal
Universiti Teknologi Malaysia

2006

Abstract

The characteristic of swirling flames produced by a rotating double concentric burner is described. The effect of rotational speed, mixture ratio and mixture velocity on the shape, dynamics and height of premixed flames is studied. The effect of tube rotational speed, fuel velocity, annular air velocity and nozzle geometry on the characteristic of nonpremixed flame is also described. The emphasis of this investigation is on the study of the influence of burner rotation on the form of the premixed and nonpremixed flames. It is shown that for premixed flame as the angular velocity of rotation increases with low and moderate velocity it buckles. Buckling becomes more prominent as the angular velocity increases and eventually the flame enters the burner. At sufficiently high rotational speeds, flame stabilization on top of the burner rim becomes impossible and the flame enters into the tube, i.e. immersed flame. Rotation shortens the flame and causes the flame to stabilize at a position nearer to the nozzle exit. Lean premixed-flames studies are conducted for low, moderate and high velocity mixtures. In low jet velocities, as the burner tube starts to rotate, the flame shape is dramatically altered. The outer flame cone is shown to become wider and shorter in height. The rotating premixed flame buckles, forming a cusp flame shape. For moderate jet flow velocities, burner rotation causes the flame to form a double cone shape with one taller than the other. Lean flames at high rotational speeds have a very dynamic appearance. Experiments are also conducted on rotating nonpremixed flames. Generally, rotation enhances external mixing in originally nonpremixed flows. Starting from an originally diffusion flames the orange flame zone first increases as the rotation starts. As the rotation is fully established, a bright blue flame replaces the orange flame.

Abstrak

Ciri api berpusar yang dihasilkan oleh pembakar putaran kembar sepusat dihuraikan. Kesan halaju putaran, nisbah campuran dan halaju campuran terhadap bentuk, dinamik dan ketinggian api pracampuran dikaji. Kesan halaju putaran tiub, halaju bahan api, halaju udara annulus dan geometri muncung ke atas ciri api bukan pracampuran juga dibincangkan. Bagi api pracampuran yang mempunyai kelajuan rendah dan serdehana, api yang dihasilkan didapati melengkok. Lengkokan didapati bertambah dengan pertambahana kelajuan putaran dan akhirnya api didapati hilang ke dalam tiub pembakar. Pada kelajuan putaran yang tertentu, kestabilan api pada atas bibir tiub pembakar adalah mustahil untuk dicapai dan pada masa ini, api cenderung untuk masuk ke dalam tiub pembakar (api tenggelam). Pada umumnya, putaran tiub akan memendekkan ketinggian api dan menyebabkan api untuk stabil pada kedudukan hampir kepada muncung pembakar. Kajian api pracampuran cair dijalankan bagi kelajuan yang rendah, serdehana dan tinggi. Bagi kelajuan jet yang rendah, apabila tiun pembakar mula berputar, bentuk api bertukar secara mendadak. Kon api luaran menunjukkan kesan melebar dan bertambah pendek. Pertambahan kelajuan menyebabkan api melengkok berbentuk mangkuk (cusp). Bagi kelajuan jet yang serdehana, putaran tiub menyebabkan api kon berkembar dengan satu puncak lebih tinggi daripada yang lain terbentuk. Api pracampuran cair bagi kelajuan putaran yang tinggi menunjukkan rupa api yang begitu dinamik. Bagi ujikaji api bukan pracampuran, putaran pada umumnya menambah kadar percampuran aliran bahan api dan udara sekitaran. Api yang pada mulanya berwarna jingga perlahan-lahan digantikan dengan api berwarna biru dengan pertambahan kelajuan putaran.

Contents

Lists of Figures

Lists of Tables

LIST OF SYMBOLS

S_L	-	Laminar flame speed
δ	-	Laminar flame thickness
d	-	Quenching distance
S_t	-	Turbulent flame speed
$\overset{\circ}{m}$	-	Mass flowrate
ρ_U	-	Unburned gas density
$\overline{A}$	-	Time-smoothed flame area
S	-	Swirl number
v_θ	-	Tangential velocity component
Φ	-	Equivalence ratio
Re	-	Reynolds number
Re_r	-	Rotational Reynolds number
X_F	-	Fuel mole fraction
N	-	Rotational speed of the inner tube
MW_i	-	The molecular weights of the species of i
N_i	-	Number of moles for species
$\overset{\circ}{Q}$	-	Volume flowrate
υ	-	Kinematic viscosity
μ	-	Dynamic viscosity
ρ	-	Density of the mixture
d	-	Inner diameter of the rotating inner tube
U	-	Mean flow velocity through the inner tube
ω	-	Rotational velocity of the inner tube
G_θ	-	Axial flux of the swirl momentum
G_x	-	Axial flux of the linear momentum
r	-	Radial distance
R	-	Radius of the rotating tube
V	-	Axial velocity

Chapter 1

INTRODUCTION

This research focuses primarily on the flame behavior from a swirl burner. Specifically, we report on the behavior of premixed and nonpremixed propane flame produced from a custom design swirl burner by means of rotating inner tube at several rotational speeds.

1.1 Swirling flows and their applications

Swirling flows occur in a very wide range of applications both in nonreacting and reacting systems. In nonreacting cases, applications include, for example: cyclone separators, spraying systems, jet pumps, and many others [1]. In combustion systems, it is applied in various systems such as gas turbines, utility boilers, industrial furnaces, internal combustion engines, and many other practical heating devices [2]. Swirling jets are used as means of controlling flames and the benefits of introduction of swirl in flame stabilizer design for industrial burners have been recognized [3-6]. Swirling flows help to increase burning intensity through enhance mixing and higher residence time. It also helps in flame stabilization by the formation of secondary recirculating flows [7-8]. Additionally, swirl that occurs in practical combustion system normally involves turbulent [9]. Flame propagation in the turbulent flow fields involves complex flame-flow

interactions. One of the basic interactions of this type is that the rotating gas flow crossing the flame front. Knowing the importance of rotating flame as one of the basis to understand complex process of flame-flow interactions several investigations on rotating Bunsen burner has been performed [10-11]. The influence of centrifugal and Coriolis accelerations on the shape, stability, and extinction limits of premixed flames was investigated [12-14]. Among other observations, it was found that flame stabilization by the burner rim is possible only at sufficiently low angular velocities. Under rapid rotation, the flame flashes back inside the burner tube [14]. Mathematical model, which described the main features of rotating flames, has been formulated and basic properties for stable flame configurations have been determined [15]. The basic influence of the burner rim hydrodynamics on stabilization of Bunsen flames has been emphasized in one study [16]. In another theoretical investigation the effect of rotation on stabilization and geometry [13] the effect of rotation on stabilization and geometry of Bunsen flames that are situated inside rotating tubes was addressed. In the study [13], it was found that the rotation of the gas tends to reduce flame stabilization since flame flashback occurs at higher values of the mean flow velocity through the burner.

1.2 Swirl stabilized flames

In the present study the effects of rotation on stabilization of two main classes of flames, premixed and nonpremixed are investigated. Premixed flames in which the reactants are completely mixed on a molecular level prior to ignition and combustion. These are kinetically controlled and the rate of flame propagation, called the burning velocity, is dependent upon chemical composition and rates of chemical reaction. Completely premixed flames are seldom found in practice for reasons of safety, (for example flashback and blow-off) and stability. Diffusion flames in which the reactants mix by diffusion into a thin flame zone, and reaction rates are diffusion controlled. They are preferred in industrial practice, gas turbines, internal combustion engines, etc. being safer since the fuel and oxidant are kept separate, as well as providing greater flexibility

in controlling flame size and shape and combustion intensity. Fuel and air may be preheated and partially premixed, with additional or secondary air supplied through a separate section of the combustor [17].

In both the premixed and diffusion flames, transfer of heat, mass and momentum play important roles. The transfer will be by molecular diffusion in laminar flames and the flow of gases follows streamlines in the flow without turbulent transport. The transfer will be by turbulent diffusion in turbulent flames and the scale and intensity of turbulence affect the burning rates. In practice the need for high combustion efficiency and intensity or high heat release rates associated with turbulent combustion requires information on physical structure of turbulent flow, flame fronts, flame generated turbulence, probability density functions, flame propagation, pollution and noise generation. The discussion leads naturally to the aerodynamic effect on combustion processes and the strong interaction between them. Flame appearance at different situations of practical interest plays important basis toward understanding the combustion process. An important system parameter, which can significantly influence the flame response, is expected to be the characteristics of burner rim because it is precisely in its neighborhood where the flame is stabilized. The understanding on flame stabilization mechanism around nozzle area is essential in burner design [18-19]. The interest of writing this dissertation is motivated mainly because of lack of understanding and description of the nature of flame stabilization at the rim of double annular rotating burner of at low degree of swirl. This information is crucial for flame stabilization mechanisms and will become the basis toward understanding a much more complex flame-flow interaction process.

Experimental studies done in the past contributed toward the studies of swirl in combustion [20-33]. The study of swirl becomes important because of its wide application in flame stabilization and enhancing combustion process. One of the most flexible setup to study swirl is double concentric burner for its flexibility in experimenting both swirling premixed and nonpremixed flames. Flame emerging from

such a burner represents a group between extreme cases of premixed flames and pure diffusion flames. These burners are widely used in the combustion processes requiring a fuel-rich mixture at the flame-front, but a stoichiometric or lean mixture further downstream so that complete combustion eventually obtained within the combustion chamber. The combustion performance of this type of flames depends heavily on the mixing capability and flowfield properties [34, 39].

1.3 Swirl flow effect and characterization

Swirl has a large effect both on inert jet and on reacting flows. In nonreacting jet, swirl affecting jet growth, entrainment and decay. In reacting flow, swirl affecting flame shape, flame size, stability and combustion intensity. These effects are largely depending on the degree of swirl imparted to the flow. Generally, this degree of swirl is called swirl number S, a nondimensional number representing axial flux of swirl momentum divided by axial flux of axial momentum, times the equivalent nozzle radius. According to Gupta et al. [1],

$$S = \frac{G_\theta}{G_x \dfrac{d}{2}} \tag{1}$$

where

$$G_\theta = \int_0^\infty \left(\rho uw + \rho\overline{u'w'}\right) r^2 dr \tag{2}$$

is the axial flux of swirl momentum, including the x - θ direction turbulent shear stress term

$$G_x = \int_0^\infty \left(\rho u^2 + \rho\overline{u'^2} + \left(p - p_\infty\right)\right) r dr \tag{3}$$

is the axial flux of axial momentum, including the x direction turbulent normal stress term and a pressure term (axial trust) and u, v, w = velocity components in (x, r, θ) cylindrical polar coordinate directions. In the free jet in stagnation surroundings, G_x and

G_θ are constants, which are invariants of the jet. By virtue of the radial momentum equation, and neglect of the term $\overline{u'^2} - \left(\overline{w'^2 + v'^2}\right)/2$, the pressure contribution to G_x can be rewritten in terms of w:

$$G_x = \int_0^\infty \left(\rho[u^2 + \left(w^2 - w^2{}_{mo}\right)/2]\right) r dr \,. \tag{4}$$

For solid body rotation plug flow is assumed at the nozzle. $\left[u = u_{mo} \;\; and \; w = w_{mo} \frac{r}{d/2} \right]$

If the pressure contribution to G_x is retained in the form of a $w_2/2$ term, but the turbulent stress are omitted, the analysis leads to:

$$G_\theta = \frac{\pi}{2} \rho u_{\mathrm{mo}} w_{\mathrm{mo}} (d/2)^3$$

$G_x = \frac{\pi}{2} \rho u^2{}_{mo} (d/2)^2 (1-(G/2)^2)$ where $G = w_{\mathrm{mo}}/u_{\mathrm{mo}}$ represents the ratio of maximum velocities measured at the exit plane. Thus, the swirl strength S can be inferred from

$$S = \frac{\frac{G}{2}}{1 - \left(\frac{G}{2}\right)^2} \tag{5}$$

Solid body rotation or plug flow assumption in equation (5) is reasonably good for G less than 0.4. But for higher degree of swirl, major portion of the flow leaves the orifice near the outer edge and axial velocity distribution deviates from plug flow assumption. This cause estimation of S in equation (5) to be too low and therefore a more physically realistic relationship is needed. Then the following is suggested,

$$S = \frac{\frac{G}{2}}{1 - \left(\frac{G}{2}\right)} \tag{6}$$

In this dissertation a more practical characterization of swirl is used. Since the swirl is based on tube rotation, the inner burner rotational speed is used as the indication of the degree of rotation.

1.4 Type of swirls

1.4.1 Low swirl

Low swirl phenomena ($S \lesssim 0.4$) typically are those for which the swirl velocity does not cause the flow structure to be drastically changed [35]. As shown schematically in Figure 1.1, jet flow with this type of swirl often results in significant lateral pressure gradients only. Compared to its nonswirling counterpart, the jet produced by low degree of swirl is wider and slower. Flames with low degree of swirl have a limited practical interest mainly due to the instability problems. But similar to any other fundamental research this low swirl phenomenon is undeniably important for providing a useful ground in modeling purposes.

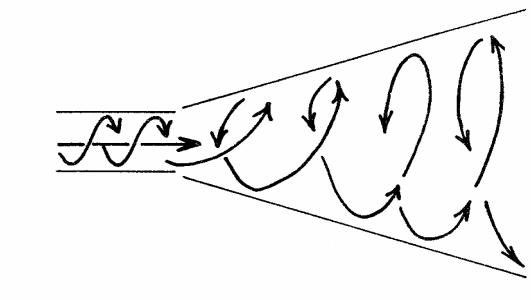

Figure 1.1: Jet flow with low degree of swirl ($S < 0.4$) resulting in significant lateral pressure gradients only. Compared to its nonswirling counterpart, the jet produced is wider and slower [1].

But there are also cases where low swirl causes change in flow structure, meaning it may possess region of recirculation. Recirculation region in low swirl application are due to geometrical constraint such as shown in the flow around bluff-body flame holders [36], 'V' gutter-type flame stabilizers, quarl or divergent nozzle, and sudden

expansions of flow cross-sectional area [37-38]. In this dissertation the emphasis has been given to low swirl and no axial recirculation zones. In some low swirl application, such as fire whirls, swirl is responsible for the lengthening of the flame, as discussed by Gupta et al. [1].

1.4.2 High swirl

At high degree of swirl ($S \geq 0.6$), radial and axial pressure gradients is large enough to cause an axial recirculation in the form of a central toroidal recirculation zone (CTRZ), which is not observed at lower degrees of swirl [39].

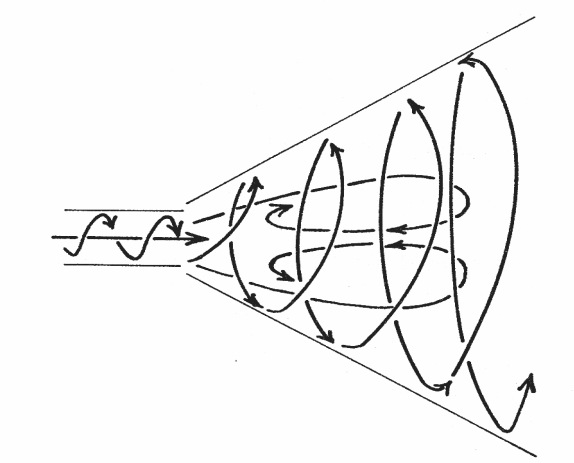

Figure 1.2: Jet flow of high degree of swirl ($S > 0.6$) resulting in significant lateral as well as longitudinal pressure gradients. Compared to its nonswirling counterpart, the jet is much wider, slower and with a central toroidal recirculation zone [1].

Shown schematically in Figure 1.2, jet flow of high degree of swirl often results in significant lateral as well as longitudinal pressure gradients. Compared to its nonswirling counterpart, the jet is much wider, slower and with a central toroidal recirculation zone. In combustion, the presence of the recirculation zone plays important role in flame stabilization by providing a hot flow of recirculated combustion products and a reduced velocity region where flame speed and flow velocity can be

matched. Swirls also act to shorten the flame length and this is advantageous for having more compact burner design [34].

1.5 Generation of swirl flow

Introducing rotation in the stream of fluid can be achieved by the following three principal methods: tangential entry of the fluid stream (axial-plus-tangential entry swirl generator), guided vanes (moving block or vane-type swirler) or simply by direct rotation (rotating tube) [1].

1.5.1 Tangential entry (axial-plus-tangential entry swirl generator)

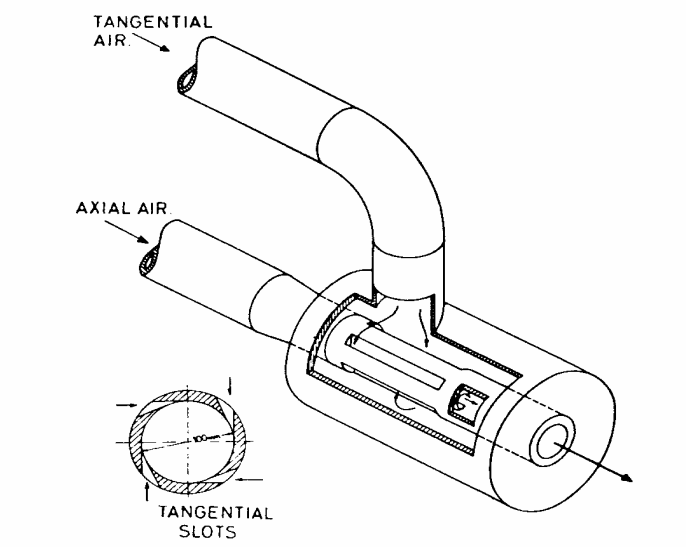

Figure 1.3: Swirl generator [40]

Figure 1.3 shows a (axial-plus-tangential entry) swirl generator that has been used for providing uniform stable jets for detailed experimental study [40]. Figure 1.4 is the sample of flame picture produced from one of the swirl generator [41]. The quantities of

air can be controlled and metered separately so that simply by adjusting the airflow rates the degree of swirl can be varied from that of zero swirl to that of a strongly swirling jet with reverse flow. Total pressure requirements of this system are relatively high, and commercial burners have tended to adopt the guided vane system, where vanes are so positioned that they deflect the flow direction [40].

Figure 1.4: Sample of flame from tangential entry swirl burner [42].

1.5.2 Guided vanes (moving block or vane-type swirler)

In radial flow into a swirl generating device, radial and tangential vane angles can be altered in situ via the movable block swirl generator, which is really akin to the tangential entry method. The movable block system, shown in Figure 1.5, is efficient in that pressure drop required for producing a certain swirl level is relatively low, and high swirl strengths are obtainable [34].

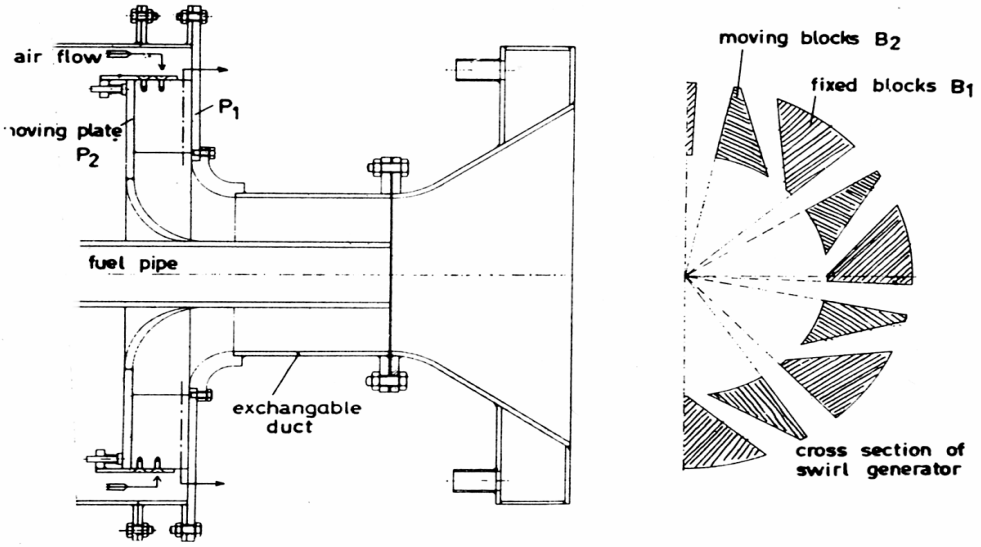

Figure 1.5: Moving block swirl burner [41].

Figure 1.6 is an example of double concentric swirl burner developed by Gupta et al. [34]. The burner consists of a central nozzle surrounded by two concentric annuli. Each annulus of the burner can be given desired swirl, either co- or counter-swirl by changing the direction of the swirler and the angle of the vane angle. The example of the flame produced from the burner is shown in Figure 1.7.

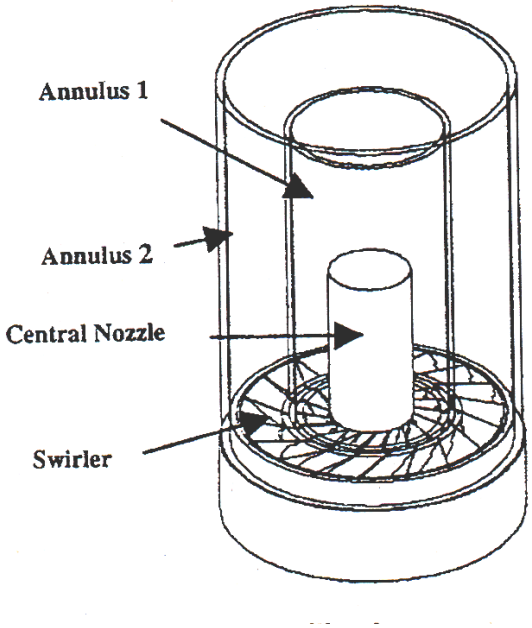

Figure1.6: Double concentric swirl burner [34]

Figure 1.7: An example of the blue flame produced from double concentric burner [34]

In axial pipe flow, shown in Figure 1.8, a vane-type swirler consists of a fixed set of vanes at certain angle to the mainstream direction, which deflects the stream into rotation. This technique is common in furnaces and gas-turbine combustors. Generally, the vanes are mounted on a central hub and the vanes occupy the space in the annular region around it. Hubless swirler has been used in an attempt to improve outlet conditions, but separation and blade stall give complex flow patterns, and axisymmetry fails [41].

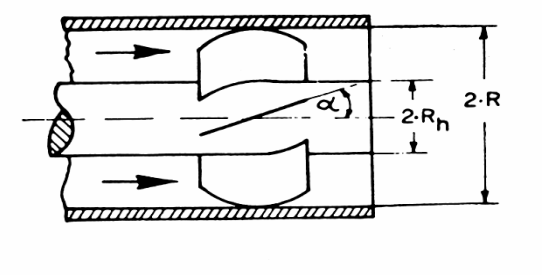

Figure 1.8: Vane-type swirler in an axial tube flow [41]

1.5.3 Direct rotation

Swirl may also be generated by direct rotation of the flow to induce a swirl motion solely by frictional drag of the cylinder wall upon the air stream passing through it. Since viscosity of air is small, the swirl effect is less seen in the fluid stream. That is why in some system, layers of honeycomb, or perforated plates or bundles of tubes are put in the middle of the rotating tubes. These kind of systems give exit velocity profiles of the 'solid body rotation' type in which the fluid particles are attached to the disk rotating with a constant angular velocity [1]. The advantage of having rotating tube is that rotation is much easier to be controlled either at low or high rotational speed. The low burner rotational speed will also enable one to see the effect it will give on the flame stabilized at very low mixture velocity. Figure 1.9 shows an example of burner setup that producing rotating flame through tube directly rotated by dc motor [15]. An example of flame picture produced from direct rotating tube is shown in Figure 1.10.

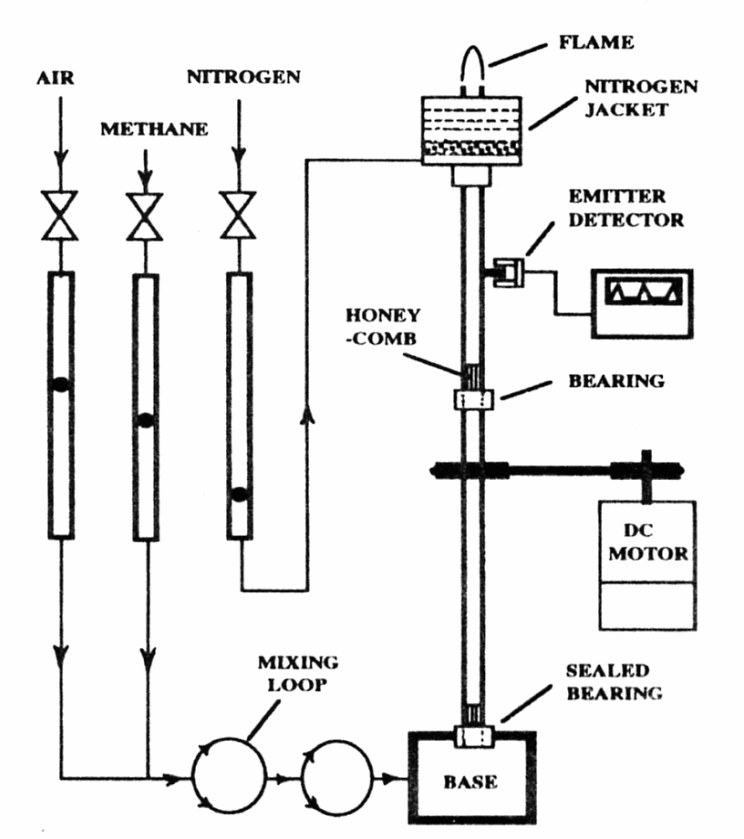

Figure 1.9: Rotating burner setup [15]

Figure 1.10: Sample picture from a rotating burner

In viscous fluid dynamics, rotating flows (that is, vortices) always possess a central core of solid body. Outside the central region, free (or potential) vortex conditions may prevail as are found in the atmosphere as whirlwinds, tornadoes, hurricanes and cyclones. Fire whirls that occur in forest and urban fires may be simulated in the laboratory by rotating a large cylindrical wire screen. Figure 1.11(a) shows the experimental setup of rotating screen for fire whirl experiment [43]. An example of the simulated fire is shown in Figure 1.11(b), and this is produced by rotating a large cylindrical wire screen with a pool of liquid fuel [36] or a gaseous jet flame [9] burning in its central vertical axis.

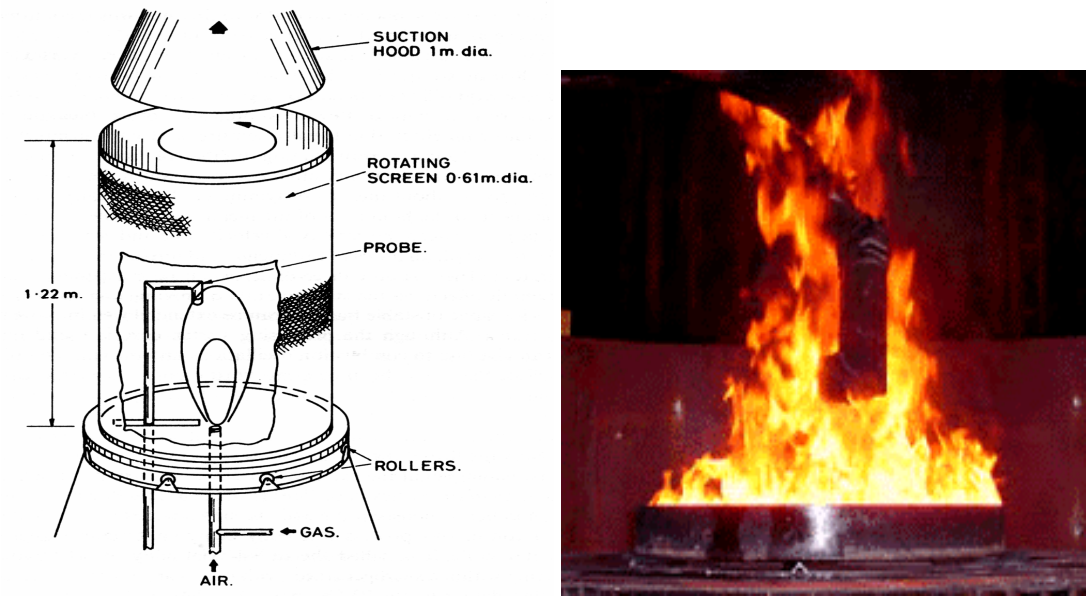

(a) (b)

Figure 1.11: Rotating screen for fire whirl experiment and the example of the fire kindled in that type of experiment [43].

Chapter 2

ROTATING BURNER SETUP, EXPERIMENTS AND ANALYSIS

2.1 Experimental Setup

The experimental setup for studying the influence of rotation on flames was design and fabricated here in the Combustion Lab, Faculty of Mechanical Engineering, UTM Skudai. The photograph of the experimental setup is shown in Figure 2.1.

Figure 2.1: The photograph of the experimental setup

The experimental setup is shown schematically in Figure 2.2 below.

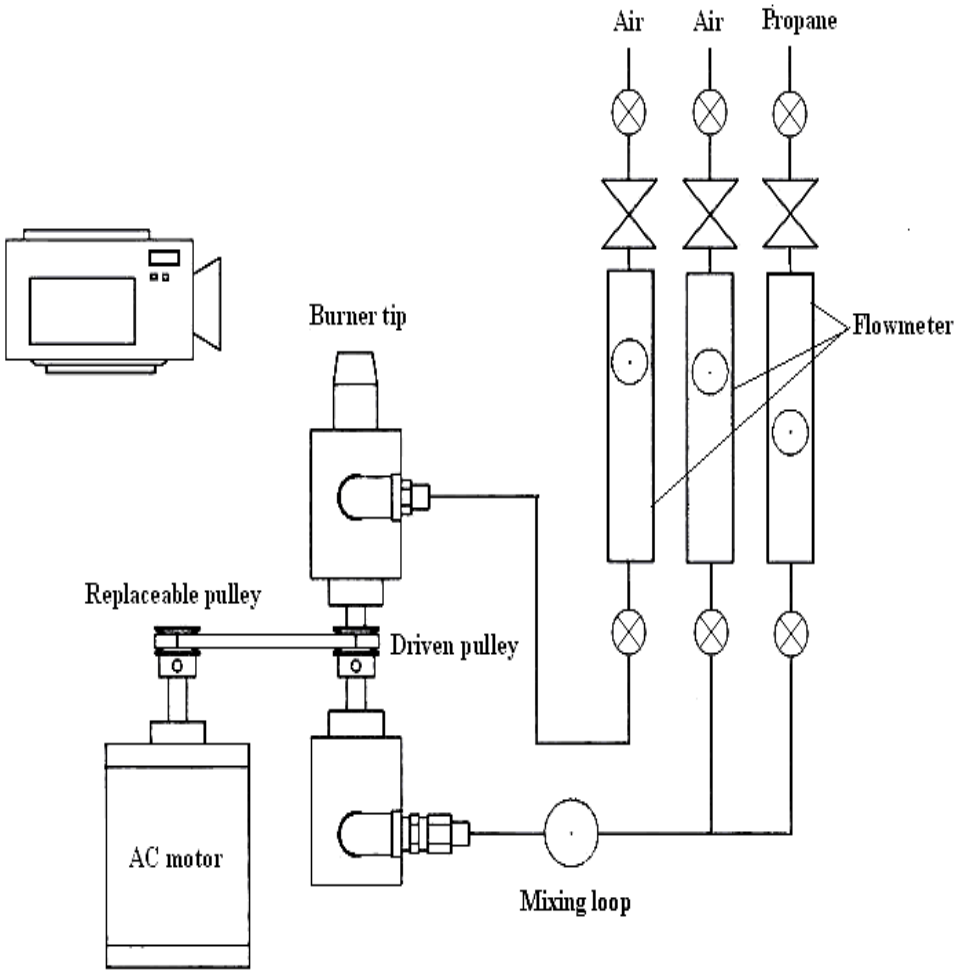

Figure 2.2: The diagram of the experimental setup

The assembly of the experimental setup is comprises of the following components:

1. Double concentric burner
2. Inner tube rotating mechanism
3. Flow control, delivery and mixing system
4. Exhaust system and protected testing area
5. Flame visualization and digitization setup

The whole burner assembly including the double concentric burner, rotating mechanism and flow control are put together and fixed on a support made of a welded iron frame with a wooden floor. The inner tube of the burner is vertically supported at bottom and at 20 mm from the rim of the burner and connected through a replaceable pulley-belt system to a motor. The pulley is replaceable in order to obtain the desired operating rotational speed. In the following sections we will discuss about the components of the experimental setup.

2.1.1 Double concentric burner

The schematic diagram of the double concentric burner is shown in Figure 2.3. The burner is comprised of several subcomponents that listed as follows:

1. Inner and outer burner tubes
2. Burner nozzle of various geometries
3. Rotating sealed contact
4. Ceramic flow straightener

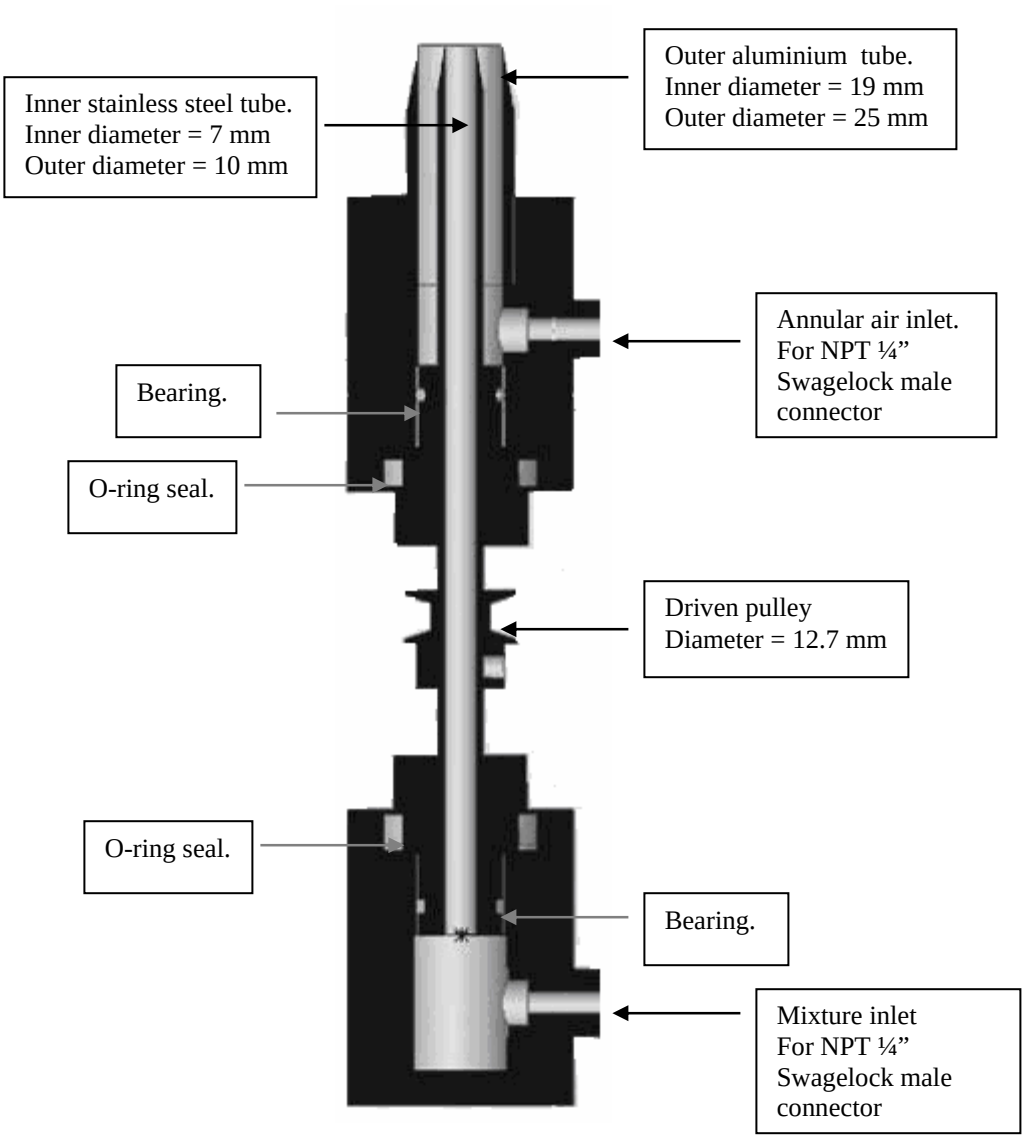

Figure 2.3: Double concentric burner assembly

2.1.1.1 Inner and outer burner tubes

The burner is made of two concentric stainless steel tubes, a rotating inner tube and fixed outer tube. The inner tube is 355.6 mm long with inner diameter of 7 mm and outer diameter of 10 mm. The outer tube is 177.8 mm long with the inner diameter of 19 mm and outer diameter of 25 mm. In order to avoid the rim effect, the tips of inner and outer tubes are tapered smoothly at about 30 degrees angle. The inner jet consists of just gaseous fuel or mixture of fuel and air and has a fixed swirl level generated by the tube rotation. Annular air is supplied through the section between the inner and outer cylinder wall and this annular air is also swirling due to the rotation of the inner tube. The combustor operates at atmospheric pressure without preheat with commercial grade propane as fuel.

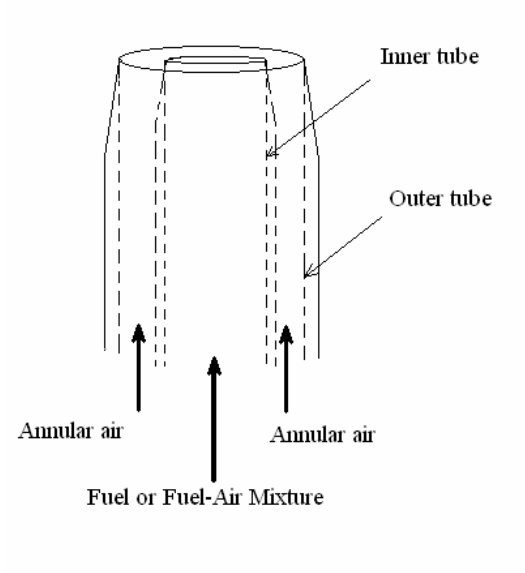

Figure 2.4: Double concentric nozzle burner

2.1.1.2 Burner nozzle of various geometries

The tip of inner cylinder is designed to be replaceable with nozzle of different geometries. There are four different nozzle configurations considered: circular, oval, triangular and rectangular.

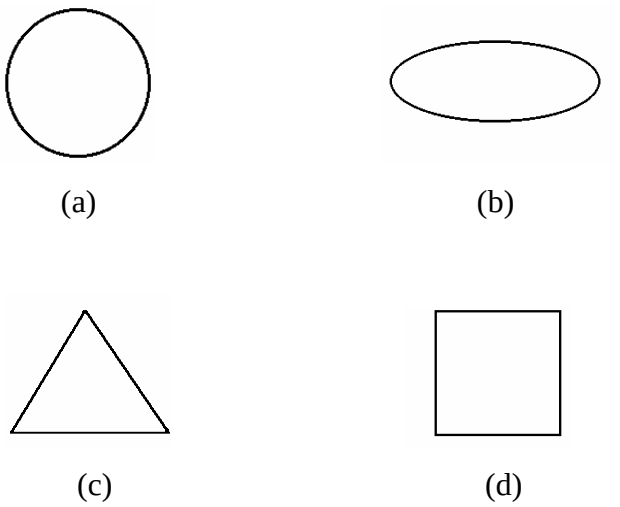

Figure 2.5: The geometrical of the nozzle burner. (a) Circular nozzle, (b) Oval nozzle, (c) Triangular nozzle, (d) Rectangular nozzle.

2.1.1.3 O-ring sealed contact

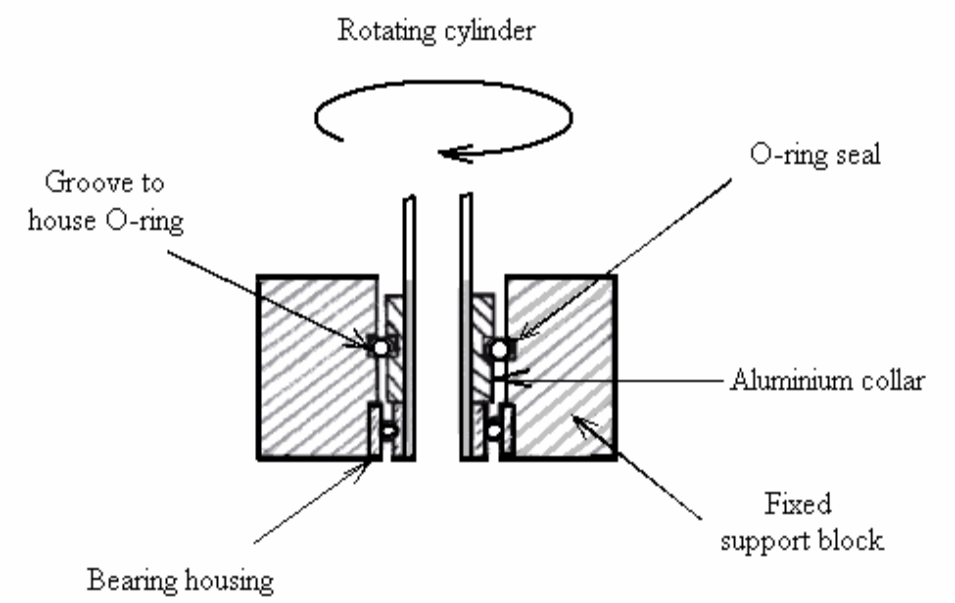

Figure 2.6: The schematic diagram of the rotating sealed contact

Another problem encountered in fabricating the experimental setup was the possibility of the leakage of the gas through the bottom section of burner tube. The possible gas leakage is due to the high velocity of fuel and air that delivered through the inner tube that rotating on the supporting blocks. In order to solve this problem an O-ring sealed contact such as shown in Figure 2.6 is designed to house the rotating inner tube on the burner block.

2.1.1.4 Ceramic flow straightener

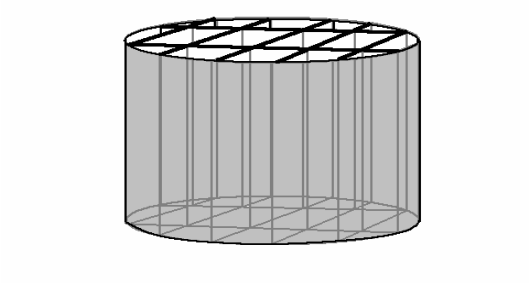

Figure 2.7: The schematic diagram of ceramic flow straightener.

In the assembly there are two locations where ceramic flow straightener is installed, one at the middle and the other is at the bottom part of the stainless steel cylinder. The purpose of having these items is for having uniform flow of fluid out of the nonrotating inner cylinder. The use of this ceramic flow straightener, such as shown schematically in Figure 2.7, is also important in generating rotating bulk flow of fluid from the rotating inner cylinder. The fluid that flowing through the inner cylinder mainly affected by the skin friction between the fluid and wall. In order for the fluid to be affected by the rotating tube the flow straightener need to be installed.

2.1.2 Inner tube rotating mechanism

Rotation of the inner burner tube is achieved through a pulley-motor mechanism (Figure 2.8) that connecting the inner tube and the motor.

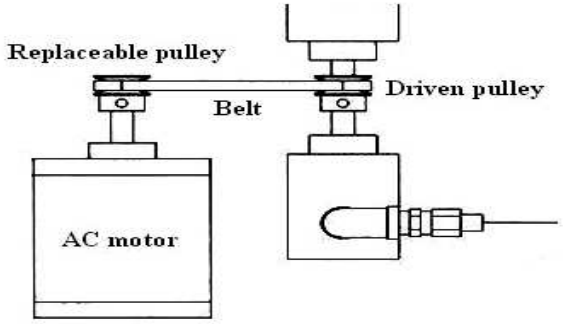

Figure 2.8: Burner tube rotating mechanism

The motor is an 1hp ac motor having a fixed rotational velocity of 1420 rpm. Different rotational velocity of burner tube is achieved by replacing different sizes of pulleys that fixed on the motor shaft. Table 2.1 shows the different rotational speed under the different size of driver pulley:

Driver Pulley	Rotational speed of the inner tube
A	**2190 rpm**
B	**2540 rpm**
C	**2640 rpm**
D	**2760 rpm**
E	**3240 rpm**
F	**4000 rpm**
G	**4500 rpm**

Table 2.1: Different rotational speed under the different size of driver pulley

2.1.3 Flow control system

The schematic diagram of the setup flow control system for the burner is shown in Figure 2.9.

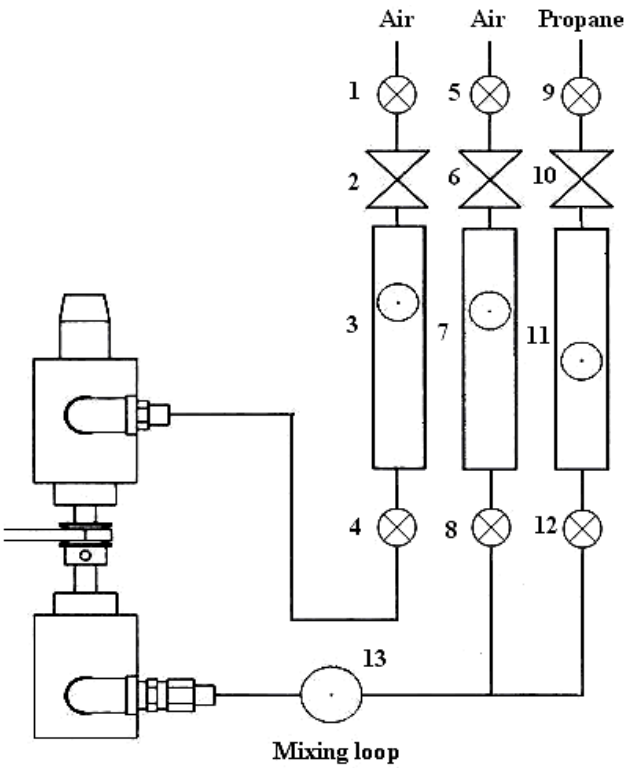

Figure 2.9: The schematic diagram of the flow control system:

1. Shut-off valve,	2. Metering valve,	3. Cole-Palmer flowmeter,
4. By-pass valve,	5. Shut-off valve,	6. Metering valve,
7. Dwyer-air flowmeter,	8. By-pass valve,	9. Shut-off valve,
10. Metering valve,	11. Cole-Palmer flowmeter,	
12. By-pass valve,	13. Mixing loop	

Air and fuel flow control system for the experimental setup consist of air source, fuel source, air flow meters, fuel flow meters, mixing loop, valves and connecting flow lines. Air source for the experiment was obtained through air compressor. Fuel source from the industrial propane tank supplied from a gas tank with $\geq$ 99.5% purity. Several valves and rotameters were used to control the amount of fuel, air and the degree of fuel-air mixing. The schematic diagram for the experimental setup is shown in Figure 2.9. The following are the flowmeters used in the setup:

1. Cole-Palmer flowmeter with the scale reading in the range of 0 to 150 mm that correspond to maximum fuel flow rate of 2200 ml/min
2. Dwyer flowmeter with the direct reading of the air flow in the range of 0 to 100 SCFH is used to control the air flow rate
3. Cole-Palmer flowmeter with the scale reading in the range of 0 to 150 mm that correspond to maximum annular air flow rate of 22000 ml/min

2.1.4 Protected experimental test section

To ensure the flame is free from outside disturbance the experiments were conducted in an enclosed area where the experimental setup was surrounded with screens made of transparent Perspex of 5 x 4 x 4 foots. The Perspex was covered with black papers to ensure dark environment for image capturing. The front section of the experimental area was covered by a black curtain for the same reason. The exhaust fan, situated at the upper section of the setup, was switched off during the experiments.

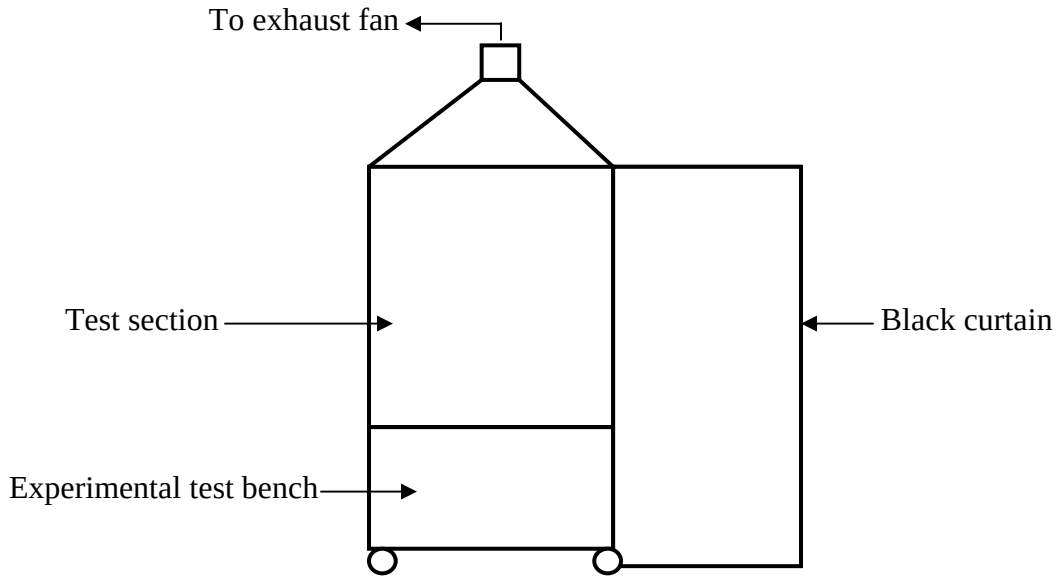

Figure 2.10: Protected experimental test section

2.1.5 Experimental procedure

The setup is designed to run two types of experiments: premixed flame and nonpremixed (diffusion) flame. For premixed flame experiment both fuel and air is allowed to mix at different proportions and then mixed thoroughly in the mixing loop prior to the introduction to the inner burner tube. For diffusion flame experiment, only fuel is metered and introduces to the inner burner tubes. In some experiments air is metered in the Dwyer air flowmeter and allowed to flow in the region between the two tubes in order to see the effect of annular air on the flame. The fuel or fuel-air mixture is then lighted up at the rim of the inner burner tube.

2.1.6 Flame visualization and analysis setup

Visualization plays a major role in this flame investigation. The investigation of the flame involves measurement of its height, pattern, color and behavior. Flame capturing, image digitization and analysis setup are shown in Figure 2.10 It consists of the following components:

1. Video camera
2. Digital camera
3. Analog to digital video converter
4. Video player
5. Computer
6. Digital film reader
7. Video displaying and editing software

Flames appearance was recorded in analog format via SONY Hi8 camcorder and JVC VHS camcorder. In this experiment the analog video source was used purposely because the digitizing will produce smaller, easier to handle video file such as MPEG-1 format compared to its Digital Video (DV) counterpart.

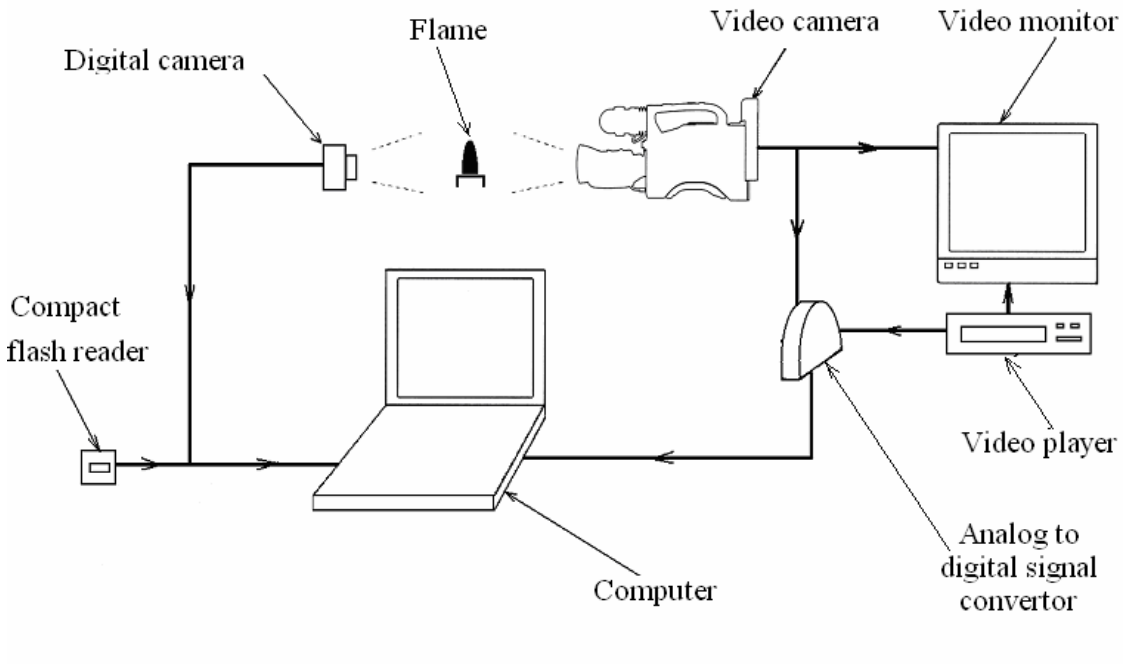

Figure 2.11: The video digitization and analysis setup

The digitization process, which converting the video from analog to digital, was performed by using Dazzle Video Capturing device. The video captured via Hi8 camcorder can be linked directly to the device whereas the video captured via JVC VHS camcorder need the video to be stored first and then played using a video player which in turn connected to the same analog to digital converter device. In the digitization process the playing video scene are shown live at the computer in the Dazzle Digital Video Creator preview window. The desired section of live video then captured and saved into digital video clips. The high-resolution images of still pictures are captured using Minolta digital camera. The Minolta S404, the 4-megapixel digital camera can be used to capture both digital still and moving scenes. Compact flash, which acts as the digital film, is used to save the pictures as well as the moving scenes.

Downloading the captured pictures can be done directly to the computer through a USB cable or can be read by inserting the compact flash in a digital film reader.

2.1.7 Data reduction

Once all the desired video scenes and pictures are stored digitally in the personal computer, the playback mode in the software is used to preview video and picture at any instant for analysis. The software enables us to preview the video clips, individually and frame-by-frame. Flame analysis is made easy by the ability of previewing the digital video at any desired instant. The digital video is captured in MPEG-1 format at a rate of 30 frames per second. For flame height determination, the digital flame picture is displayed individually and the blue flame tip is recorded as the flame height. For measurement purposes, a scale that is based on the inner tube diameter is put at the background during the experiment. Based on the average of the height over certain appropriate duration is recorded. This feature gave one the flexibility to review the flame at any instant that deserves attention. With this, the flame shape, color, intensity as well as flame height were being able to be determined in a discrete manner.

Chapter 3

PREMIXED FLAME

3.1 Premixed flame characteristics

3.1.1 Introduction

An extensive study on the flame characteristics of swirl jet is performed. In this study, we have considered the effect of several parameters on the flame shape, color, stability, and height. The parameters considered are: rotational speed of the internal tube, equivalence ratio of internal gas mixture, velocity of mixture, annular air velocity and nozzle geometry. The following discussion is divided into three parts. In the first part we discussed shapes of rotating premixed flames, second, rotating diffusion flames and third, rotating flames from burner of various nozzle geometries.

3.1.2 Rotating lean premixed flames

Lean premixed flames are categorized into three parts: low, moderate and high velocity jet flames. Each has its own specific characteristics depending on mixture equivalence ratio and burner rotational speed. Figures 3.1.1 (a and c) show pictures of a premixed

flame without rotation, with low jet velocity (43 cm/s) and equivalence ratio of ϕ = 0.59. Both pictures are for the same flame except the second one (Figure 3.1.1 c) is the inverted color of the first one (Figure 3.1.1 a). The inverted picture is produced for a better look of the flame structure. The inner cone of the flame is distinguished by a bright blue flame with an open tip. Surrounding the inner cone is a bright blue sheath, or called outer cone, extending from the bottom to the flame tip. Here the outer cone stands in a close vicinity of the inner cone. The outer cone is due to the carbon monoxide produced from the rich inner flame. The combined effects of velocity profile, flame speed, and heat losses to the tube wall determine the shape and color of the flame.

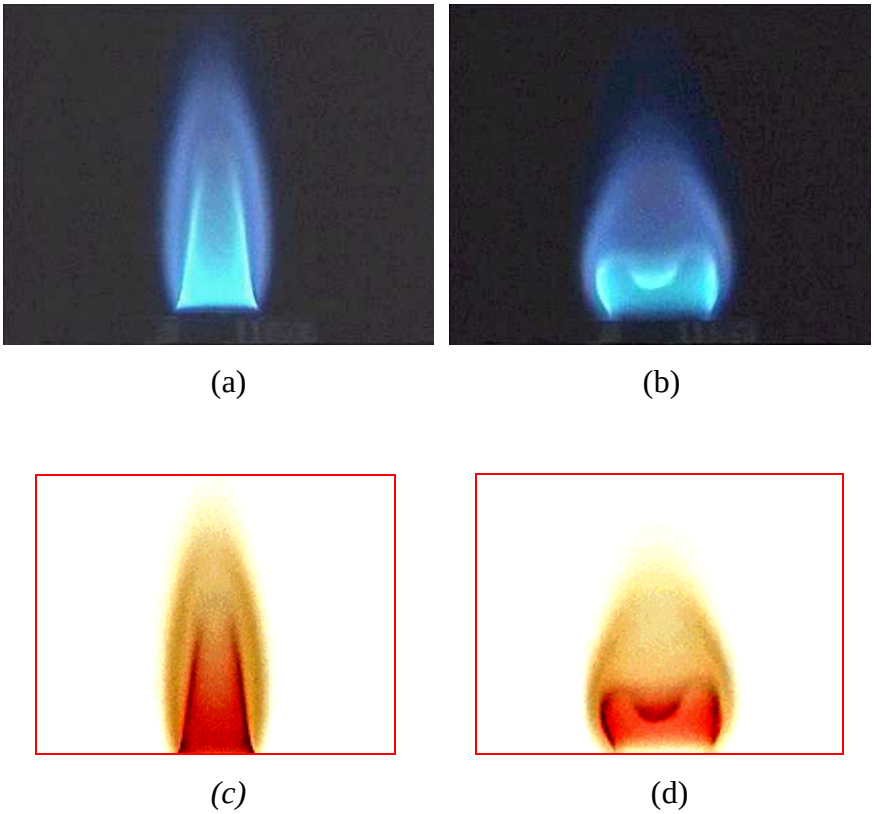

(a) (b)

(c) (d)

Figure 3.1.1: The effect of rotation on lean premixed flame, ϕ = 0.59 and V = 43 cm/s.
(a) Stationary (b) Rotating with the speed of 3240 rpm.
(c) Color inverted picture of (a). (d) Color inverted picture of (b).

Once the burner tube starts to rotate, the flame shape is dramatically altered as shown in Figures 3.1.1 (b and d). The flame is buckled forming a cusp shaped flame. The outer flame cone is shown to become wider and shorter in height, following the shape of the inner cone. The velocity profile at the exit of the rotating tube is depicted in Figure 3.1.2. The flame buckling occurs due to reduced axial flow velocity at the central part of the inner tube. The flame location in a premixed flame is where the flame speed S_L is balanced with the local gas velocity. It can be clearly seen, from Figure 3.1.2 that the flame tends to move upstream at the central part of the tube.

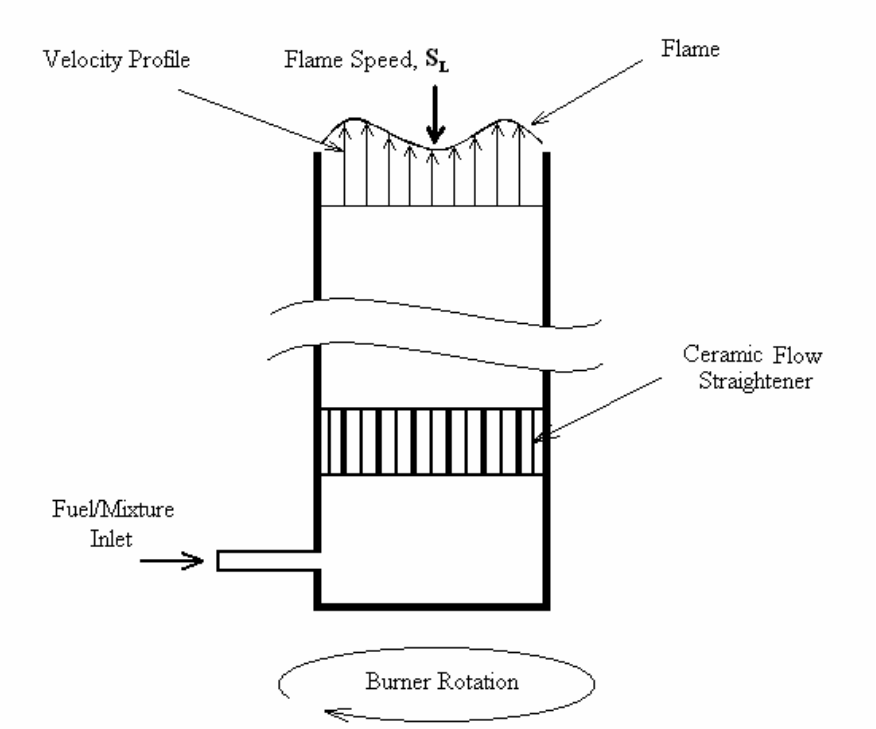

Figure 3.1.2: Schematic diagram of low flow velocity subjected to the rotation of burner inner tube.

The effect of increasing flow velocity of the mixture in moderate regime (ranging from 70 to 120 cm/s) is shown in Figure 3.2.3 (a), which shows a closed tip flame for mixture velocity of 93.3 cm/s. The increasing velocity supplies a sufficient amount of fuel-air mixture for complete combustion thus forming closed tip flame with no outer cone.

Nonrotating *ω = 2540 rpm*

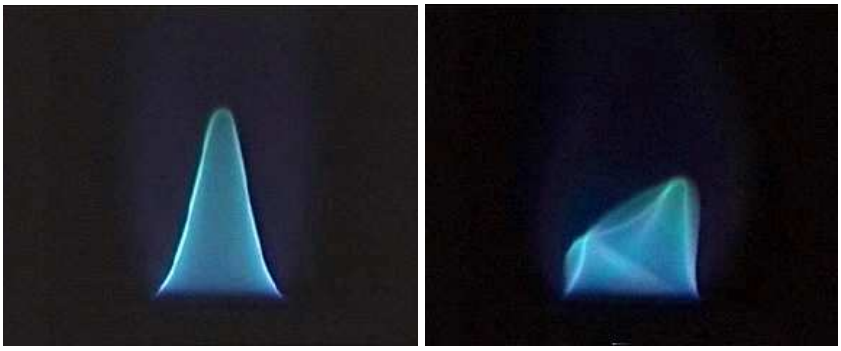

(a) (b)

(c) (d)

Figure 3.1.3: The effect of rotation on lean premixed flame: ϕ = 0.59 and V = 93.3 cm/s.

(a) Stationary flame:Without rotation. (b) Transitional flame:ω =2540 rpm,

(c) Color inverted picture of (a), (d) Color inverted picture of (b).

Her

For the stationary case, the flame appears stable with dark blue color in the core and brighter whitish blue color bordering the flame surface. This is a typical lean premixed flame for a rotating tube with speed of 2540 rpm; a transitional flame shown in Figure 3.1.3 (b) appears. As the burner tube rotates, the flame wiggles and shows a double tip appearance. One tip is higher than the other. It is also noticed that the flame height reduces to almost 2/3 of its non-rotating height. The buckled flame with double tips is shown clearly in the color-inverted image of Figure 3.1.1 (d) where the tips seem to be connected together. The velocity profile at the exit of the rotating tube at this velocity is depicted in Figure 3.1.4. The fuel-air mixture enters the burner inner tube at 90 degrees angle. Even though there is a ceramic flow straightener, the combined effect of tangential flow entry at high velocity and tube rotation causes the flow velocity at the burner exit to deform as shown in Figure 3.1.4.

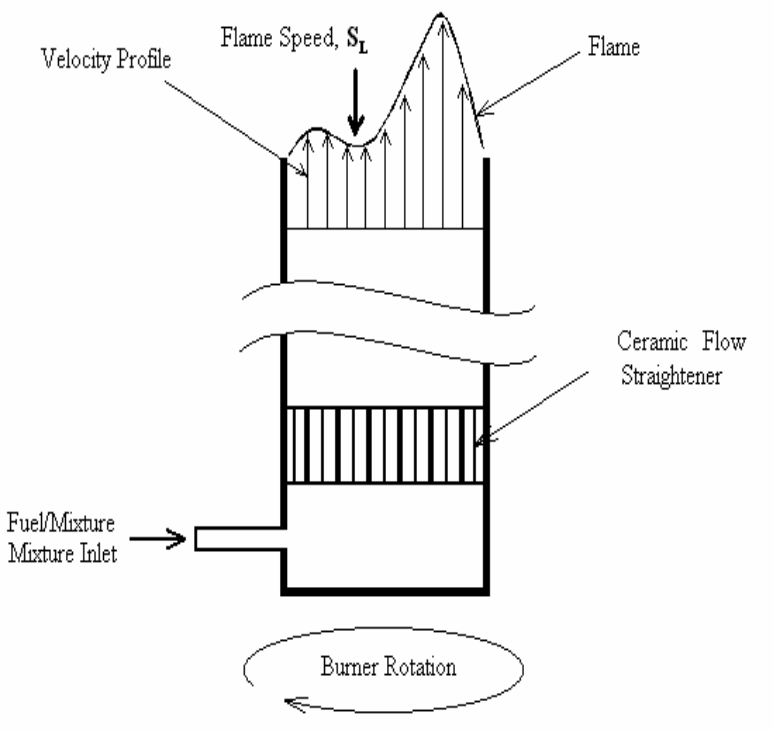

Figure 3.1.4: Schematic diagram of high flow velocity subjected to the rotation of burner inner tube.

Next, the tube rotation is increases to a higher speed of 4500 rpm. Since the rotational speed is almost doubled, yet the shutter speed is kept the same, the flame picture shown in Figure 3.1.5 has two superimposed images. The video camera uses 1/30 sec shutter, whereas tube rotational speed is more than 1/60 sec. Therefore at least, two superimposed images of the flame are shown in 3.1.3 (b).

The centrifugal force due to inner tube rotation also causes the flame tips to point outward, about 30 degrees with respect to its vertical axis. Compare to the stationary flame shown in Figure 3.1.3 (a), the flame height in Figure 3.1.5 is shorter by about 1/3 of its original height.

A very lean flame, $\phi = 0.22$, having moderate mixture velocity of 92.5 cm/s is shown in Figure 3.1.6. In the stationary case, Figure 3.1.6 (a), the balance between the flow velocity and flame speed of very lean mixture end up with a stable, relatively shorter flame. The fuel-lean mixture producing a bluish white flame, the color that is much lighter than the other flames shown earlier.

(a) (b)

Figure 3.1.5: The effect of rotation on lean premixed flame: $\phi = 0.59$ and V = 93.3 cm/s.

(a) Rotating with the speed of 4500 rpm, (b) Color inverted picture of (a).

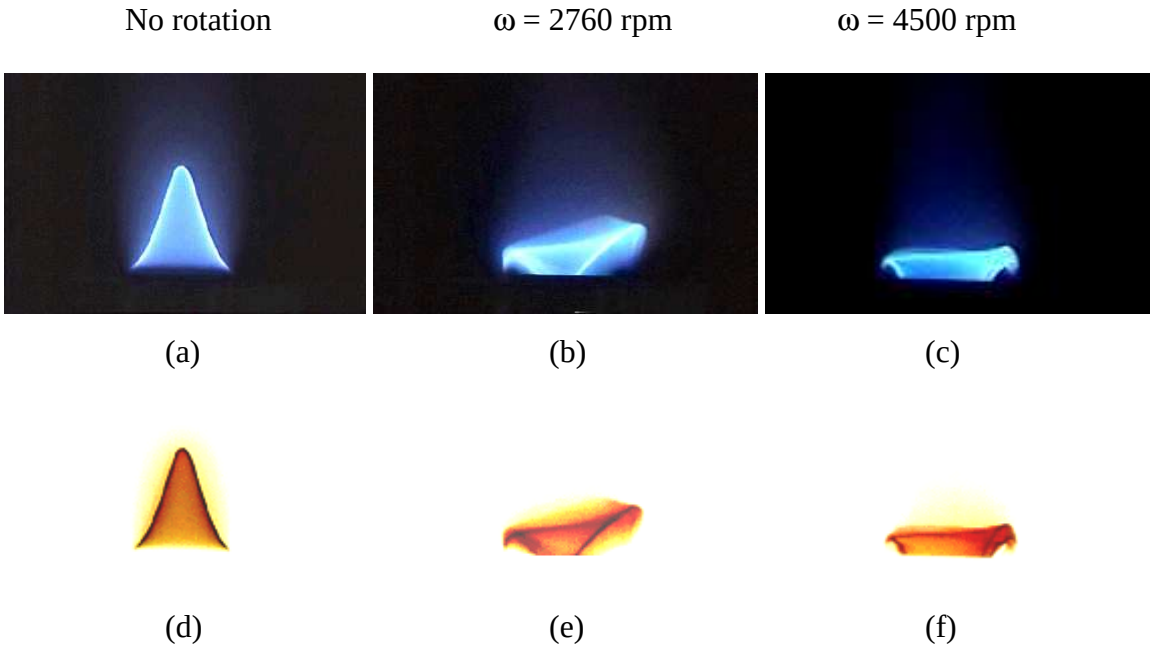

Figure 3.1.6: Flame pattern as the rotational speed increases. The corresponding premixed flames is having low flow velocity and very lean mixture: $\phi = 0.22$ and V = 92.5 cm/s.

(a) Stationary flame, (b) Rotated at ω = 2760 rpm,

(c) Rotating at ω = 4500 rpm, (d) Color inverted picture of (a),

(e) Color inverted picture of (b), (f) Color inverted picture of (c).

As the burner inner tube is rotated at 2760 rpm the flame start to buckle with its tip starts to immerse into the burner tube. The outer cone appears very dim indicating significant mixing with the ambient. When the burner rotational speed is further increased to 4500 rpm the premixed is flame further sucked into the burner tube with a shape shown in Figure 3.1.6 (c). The color inverted images of every picture are shown in Figure 3.1.6 (d), (e) and (f). The flame outer cone is totally gone indicating complete combustion of the fuel in the inner cone section.

Several interesting features of premixed flames with moderate mixture velocity of 94 cm/s, equivalence ratio of 0.89 and at different burner rotational speed are provided in Figure 3.1.7. Without rotation the conical flame, shown in 3.1.7 (a) is steady, and has a typical bright bluish color and a brighter flame boundary or flame surface. As the rotation is introduced, the flame cone appears to become unsteady and start to wiggle around the burner rim. Figure 3.1.7 (b), shows that the tip of the flame starts to buckle when the burner rotational speed reaches 3240 rpm. As the rotational speed is further increased to 4000 rpm, the flame tends to buckle much more with intermittent wrinkles (Figure 3.1.7 (c)).

Premixed flames with moderate mixture velocity of 94 cm/s equivalence ratio of 0.54 rotated at different rotational speed ranging from stationary to 4500 rpm are shown in Figure 3.1.8. Here the mixture velocity is again fixed at velocity of 94 cm/s.

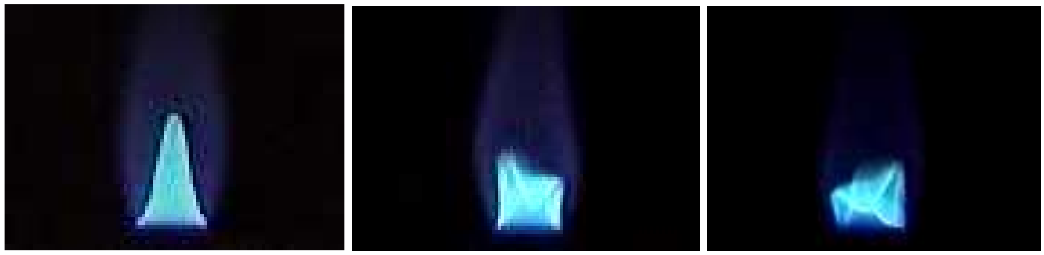

(a) ω = 0 (b) ω = 3240 rpm (c) ω = 4000 rpm

Figure 3.1.7: Premixed flames at different rotational speed: Mixture velocity, V = 94 cm/s, ϕ = 0.89.

(a) Stationary (b) ω = 2540 rpm (c) ω = 3240 rpm (d) ω = 4500 rpm

Figure 3.1.8: Premixed flames at different rotational speed. Mixture velocity, V = 94 cm/s, ϕ = 0.54.

As seen earlier (Figure 3.1.7), tip buckling starts to occur as the speed reaches 2540 rpm. In this rotational speed the tip buckling causes the overall flame height to reduce to almost half of its original height. For the speed of 4500 rpm the flame appears more like tulip shape with double layers of curving down flame sheets stacked on top of each other. This interesting appearance of the flame is mainly due to the competing speed between the flame propagation going downward and flow that is going upward. In this particular experiment if one were to consider the mixture to be always constant, then the flame speed is always constant too. The changing flame pattern therefore is just because of the changing velocity profile at the outlet of the burner with the possible tube vibrational effects especially towards the burner rim. But there is possibility also for the mixture to get more mixed as the rotational speed increases as a result the mixture at the outer section, the section which is exposed to the ambient air get more mixed, and becomes more lean.

The flame characteristics in high flow velocity regime are described next. Pictures in Figure 3.1.9 show the effect of rotation on the lean premixed flame having an equivalence ratio of 0.42 and high mixture velocity of 275 cm/s. As the mixture flow velocity is increased, the need for the balance between flame speed and flow velocity causes the flame to become taller with a light blue color. Figure 3.1.9 (a) shows a bright blue outline bordering the flame cone. Burner rotation for this kind of flame is not expected to cause buckling. Indeed, as shown in Figure 3.1.9 (b), the flame shakes vigorously on its burner rim as the tube rotates at a speed of 2540 rpm. The flames for low and high rotational speeds basically show little difference. Both flames, Figures 3.1.9 (b) and (c), show a very dynamic appearance, in which the flame dances from one side to the other.

(a) Stationary *(b) ω = 2540 rpm* *(c) ω = 4500 rpm*

Figure 3.1.9: Effect of rotation on fuel-lean (ϕ =0.42) flame occurs at low and high rotational speed.

(a) (b) (c)

ϕ = 1.1
V = 43.7 cm/s

ϕ = 0.56
V = 64.7 cm/s

ϕ = 0.5
V = 75.8 cm/s

(d) (e) (f)

$\phi = 0.39$	$\phi = 0.3$	$\phi = 0.28$
V = 89.7 cm/s	V = 121.5 cm/s	V = 125.6 cm/s

Figure 3.1.10: Effect of air dilution on the shape of rotating flames.

Changing mixture velocities from low to high by diluting more air on a fixed fuel flow for rotating burner is discussed next. Figure 3.1.10 shows the change of flame pattern due to air dilution on the premixed flames rotated with fixed rotational speed of 4000 rpm. Dilution causes the equivalence ratio to decrease. For example as the mixture velocity increases from 43.7 cm/s to 125.6 cm/s, the equivalence ratio decreases from 1.1 to 0.28 and the flame appears to change in shape and color from Figure 3.1.10 (a) to Figure 3.1.10 (b). Their inverted images are shown in Figure 3.1.11 (a) and (b) respectively.

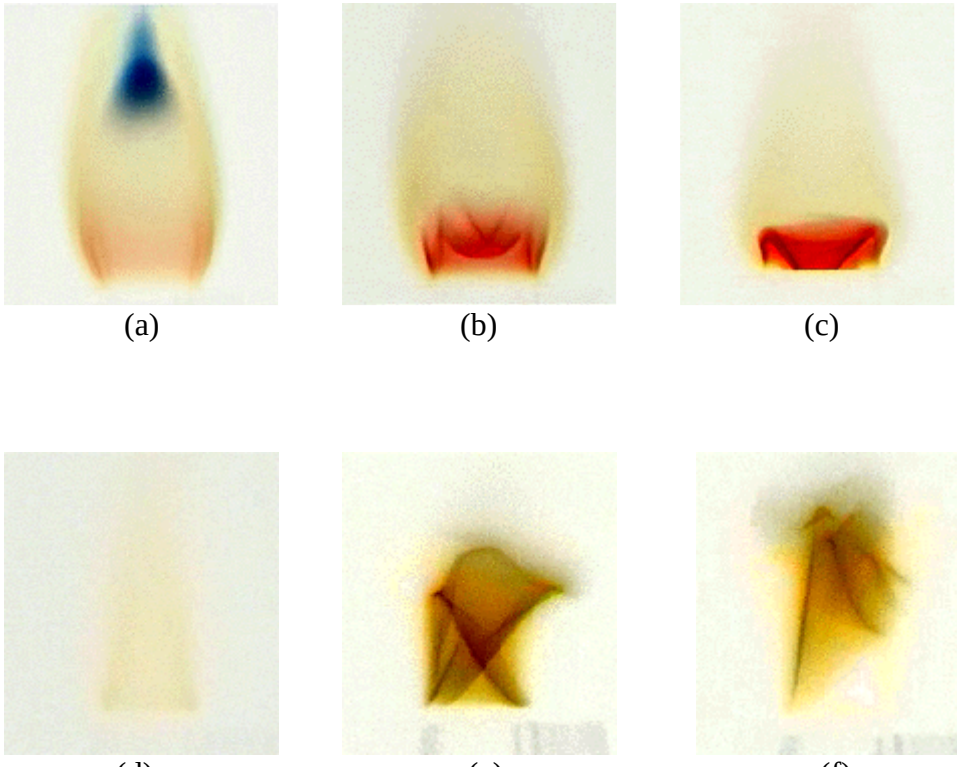

(a) (b) (c)

(d) (e) (f)

Figure 3.1.11: The color inverted images of flame in Figure 3.2.10 showing the effect of air dilution on the shape of rotating flames. Burner rotational speed,

ω = 4000 rpm. Propane gas fixed at 0.12 scfh and air is added gradually

(a) ϕ = 1.1, V = 43.7 cm/s, (b) ϕ = 0.56, V = 64.7 cm/s

(c) ϕ = 0.5, V = 75.8 cm/s, (d) ϕ = 0.39, V = 89.7 cm/s

(e) ϕ = 0.3, V = 121.5 cm/s, (f) ϕ = 0.28, V = 125.6 cm/s.

Figure 3.1.10 (a) shows the flame for the equivalence ratio of 1.1 and mixture velocity 43.7 cm/s. The flame is slightly rich with deep violet blue and orange tip color. The orange tip is shown to have a small soot wing penetrating on top of its tip. When the air is added the mixture becomes fuel-lean until a velocity of 64.7 cm/s is reached in Figure 3.1.11 (b). This flame shows an interesting look with the inner cone starting to buckle. The buckling in this case however, oscillates vigorously. The increment of mixture velocity does not increase the overall flame height. The reduction of equivalence ratio decreases the flame speed and it is supposed to increase the flame height. However, the flame height decreases. This is because the burner rotation, which in effect causes the flame tip to buckle, dominates the overall flame shape. As the airflow increases and the mixture velocity reaches 75.8 cm/s and the equivalence ratio reduces to 0.5, the flame tip buckles into the burner mouth (Figure 3.1.10(c)). As the air is added until the mixture becomes 0.39, the flame is completely immersed into the burner tube (Figure 3.1.10(d)). As more air is added until the mixture velocity reaches 121.5 cm/s and the equivalence ratio is lowered to 0.3, the flame is reemerged back out of the burner tube, as shown in Figure 3.1.10(e)). In this figure, the flame dances violently with a whitish purple color. At this condition, the mixture velocity and further reduction of flame speed play a dominant role over the rotational effect and push the flame to become taller. Eventually, as soon as the flame velocity reaches 125.6 cm/s and the equivalence ratio drops to 0.28, the flame dances much more vigorously until it is blown away from the burner rim (Figure 3.1.10(f)).

3.1.2.1 Effects of annular air on lean premixed flames

In this section the effect of an annular air applied on the rotating lean premixed flames is discussed. Two categories of flow are considered: low velocity and moderate velocity jet flames.

$V_{aa} = 0$ $V_{aa} = 35.5$ cm/s $V_{aa} = 142$ cm/s

(a) (b) (c)

(d) (e) (f)

Figure 3.1.12: The effect of annular air on premixed flames: ϕ = 0.48, V = 50 cm/s and ω = 3240 rpm.
(a) V_{aa} = 0, (b) V_{aa} = 35.5 cm/s, (c) V_{aa} = 142 cm/s,
(d) Invert image of (a), (e) Invert image of (b), (f) Invert image of (c)

Figure 3.1.12 shows a low velocity jet flame subjected to increasing annular air and burner rotation. The flame mixture equivalence ratio is 0.48 flowing at a velocity of 50 cm/s and constant inner tube rotation of 3240 rpm. In Figure 3.1.12 (a) no annular air is applied and the flame inner cone buckles. The flame is blue in color showing two regions; bright inner and outer cone. In Figure 3.1.12 (b), as the annular air of 35.5 cm/s is applied, the flame inner cone still buckles. However, the inner cone is shown to shrink in size but with a gain in height. Here, the application of an annular air increases mixing, reducing equivalence ratio and hence lowers the flame speed. As a result, the flame height increases. A schematic of low flow velocity subjected to an annular air is shown in Figure 3.1.13.

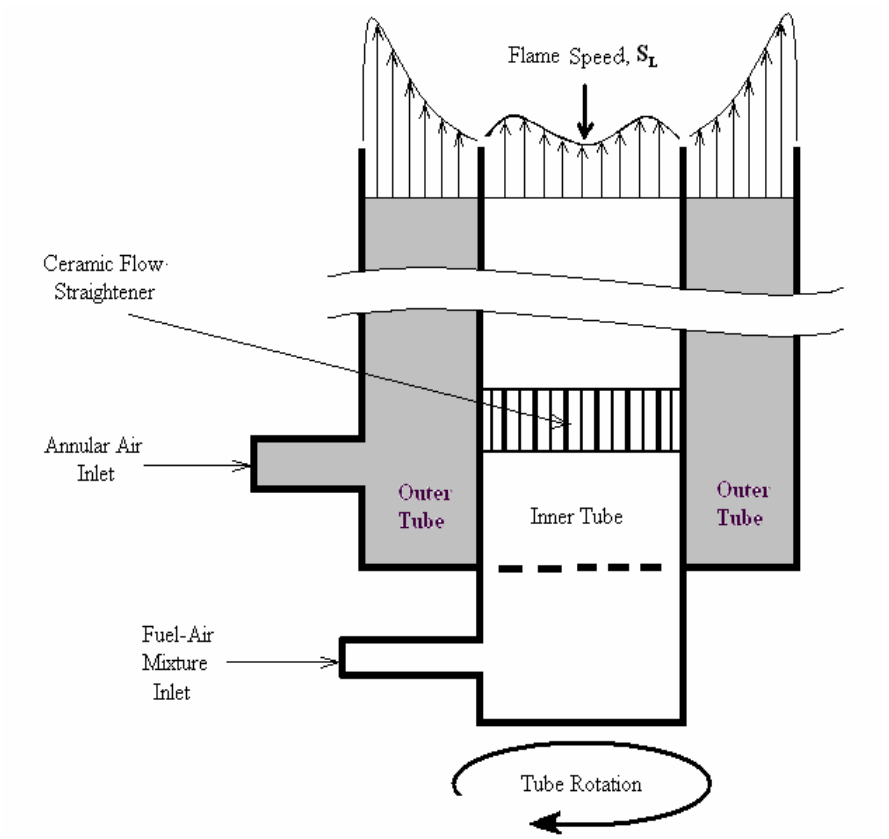

Figure 3.1.13: Schematic diagram of fuel-air flow velocity with annular airflow subjected to the rotation of inner burner tube.

Increasing the annular air to 142 cm/s further increases the flame height. The forward thrust of the fuel-air mixture overcomes the tip buckling effect, making the flame similar to a regular cone flame (Figure 3.1.12 (c)). But as the regular cone shape appears, the tube rotation causes the flame tip to wiggle. Numerous overlapping cones are observed. The skirt around the inner cone in Figure 3.2.12 (c) is just a long time exposure of a rotating cone on the edges of the flames.

The effects of increasing annular air on rotating premixed flames for moderate mixture velocity is shown in Figure 3.1.14. In this situation the fuel-gas is fixed at equivalence ratio of 0.39 and burner rotational speed of 3240 rpm.

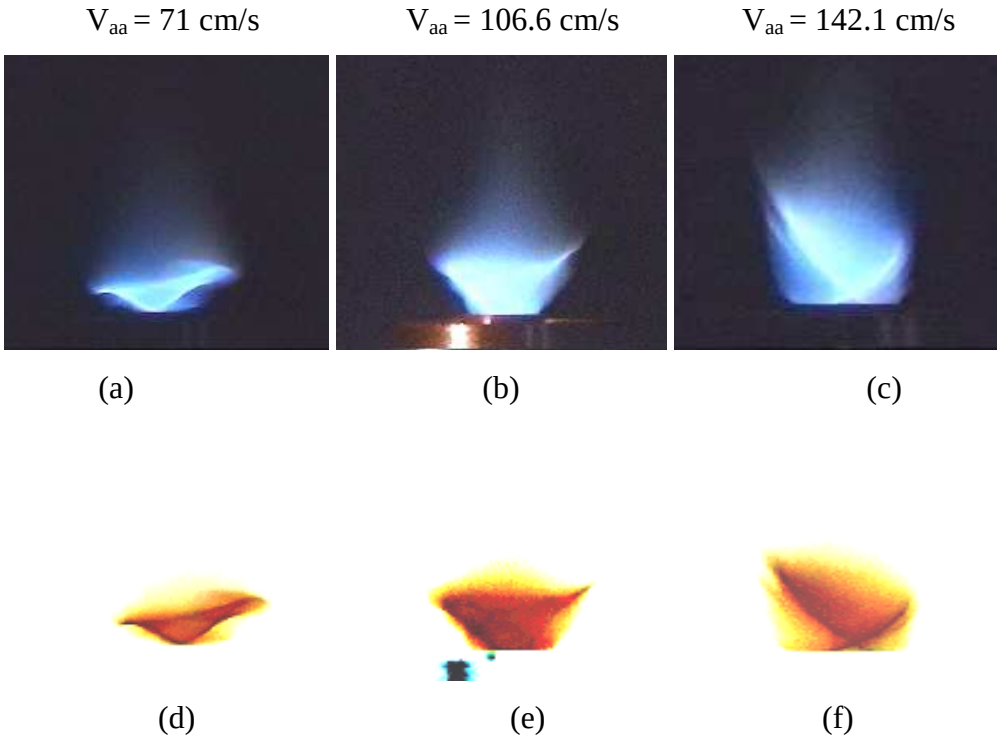

Figure 3.1.14: Effect of increasing annular air on rotating premixed flames. ϕ = 0.39,

V = 92.5, ω = 3240 rpm.

(a) V_{aa} = 71 cm/s, (b) V_{aa} = 106.6 cm/s, (c) V_{aa} = 142.1 cm/s,

(d) Invert image of (a), (e) Invert image of (b), (f) Invert image of (c)

The flame in Figure 3.1.14 is much more dynamic compare to the flame shown in Figure 3.1.12. In Figure 3.1.14, the mixture equivalence ratio is small and the flow velocity is high. Reduction of equivalence ratio reduces the flame speed and at fixed flow velocity the flame tends to move downstream. Higher flow velocity further moves the flame location downstream. However tube rotation pushes and buckles the flame tip back to the burner mouth. At this setting, the application of annular air stretches the flame upward. As the annular air increases from 71 cm/s (Figure 3.2.14 a) to 142.1 cm/s (Figure 3.1.14 c), the flame stretches further upward showing a bigger and taller wiggling flame. It appears that in Figure 3.1.14 c, increasing annular air to 142.1 cm/s increases mixing, hence, producing a brighter blue flame.

3.1.3 Rotating rich premixed flame

(a) (b)

Figure 3.1.15: Rich premixed flame with ϕ = 2.2, V = 25 cm/s, ω = 2760 rpm. (a) nonrotating, (b) rotating with ω = 2760 rpm.

Figure 3.1.15 shows pictures of rich premixed flame anchored on top of the circular nozzle burner, having an equivalence ratio of 2.2 and a mixture velocity of 25 cm/s. Figure 3.1.15 (a) is the picture of rich premixed flame without rotation. The flow in the burner tube is considered laminar, thus the velocity across the tube is parabolic in nature. The flow velocity near the burner wall is very low. This fact, as well as the heat losses to the burner rim becomes a major factor for the flame to stay stable on the top of the burner. This flame has two visible luminous zones. The rich flame shown in this figure has two distinct appearances, violet blue radiation in the bottom section and yellowish orange radiation at the upper section. Generally the appearance in the blue flame is due to the radiation from excited CH radicals, whereas, the yellowish orange is due to the presence of solid carbon particles. The dark zone in the middle section of the blue area is the region containing the unburned gas-air mixture before they enter the luminous zone where reaction and heat release take place. The bright blue stripes on the

sides of the flame are that portion of the reaction zone in which the temperature is the highest.

Figure 3.1.15 (b) shows the effect of burner tube rotation on the rich premixed flame. For a rotating flame with the speed of 2760 rpm, the lower portion of flame bulges and hence the overall flame height shortens. Burner rotation enhances the mixture mixing with the surrounding ambient air hence the oxidation rate increases. It is noticed that the blue region of the flame is affected by the burner rotation much more than the luminous orange region. One of the reasons is that the blue flame zone is normally formed in the region closer to the burner rim.

The effect of rotation and application of annular air on slightly rich premixed flame is shown in Figure 3.1.16. Starting with nonrotating case, as shown in Figure 3.1.16 (a), the slightly rich premixed flame appears to have a dark blue color with small orange tip. For a rotational speed of 3240 rpm, the lower section of the flame shown in Figure 3.1.16 (b) starts to bulge and the orange tip grows. Figure 3.2.17 shows rotation reduces the blue flame height.

(a) (b)

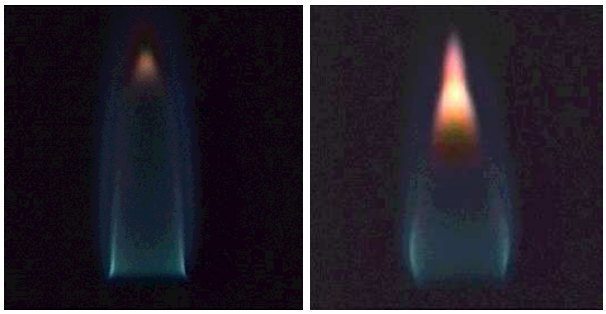

Figure 3.16: Rich premixed flame with ϕ = 2.2, V = 25 cm/s, (a) nonrotating, (b) rotating with ω = 2760 rpm.

(a) (b) (c) (d)

Figure 3.1.17: Effect of coaxial air on rotating premixed flame, ω = 3240 rpm. Slightly rich premixed case, ϕ = 1.25, V = 29.7 cm/s.
(a) V_{aa} = 36 cm/s, (b) V_{aa}= 53 cm/s, (d) V_{aa} = 107 cm/s, (e) V_{aa} = 142 cm/s.

Series of flames shown in Figure 3.1.17 are at similar condition as those in Figure 3.1.16 but with an annular air. The annular air increased from low velocities to high velocities from 36 cm/s to 107 cm/s. Annular air is introduced at 36 cm/s. This causes the bottom blue flame to wiggle sideways. The rotation and induction the annular air cause the blue flame region to become shorter, whereas, the orange flame tip becomes smaller due to increase in fuel-air mixing. As the annular air increases to 53 cm/s the flame (shown in Figure 3.1.17 (b)), appears to be totally blue, with it side surface fluctuates further. The flame rotates and fluctuates vigorously and the flame looks like skinning off to several layers starting from its bottom. The annular air fluctuates as it exits between the inner and outer tube. The skin friction of the rotating inner tube causes the annular air to rotate and when it hits the flame surface, the already spinning flame start to vibrate even more. The centrifugal force imparted by the annular air on the rotating flame surface causes certain area of the flame to shoot out of the flame surface, such as shown in Figure 3.1.17 (c). The further increases in the annular air to 107 cm/s causes the flame to lift off. Here the flow velocity already exceeds the combustion wave velocity until it reaches the equilibrium point, which in this case is several centimeters on top of the burner rim.

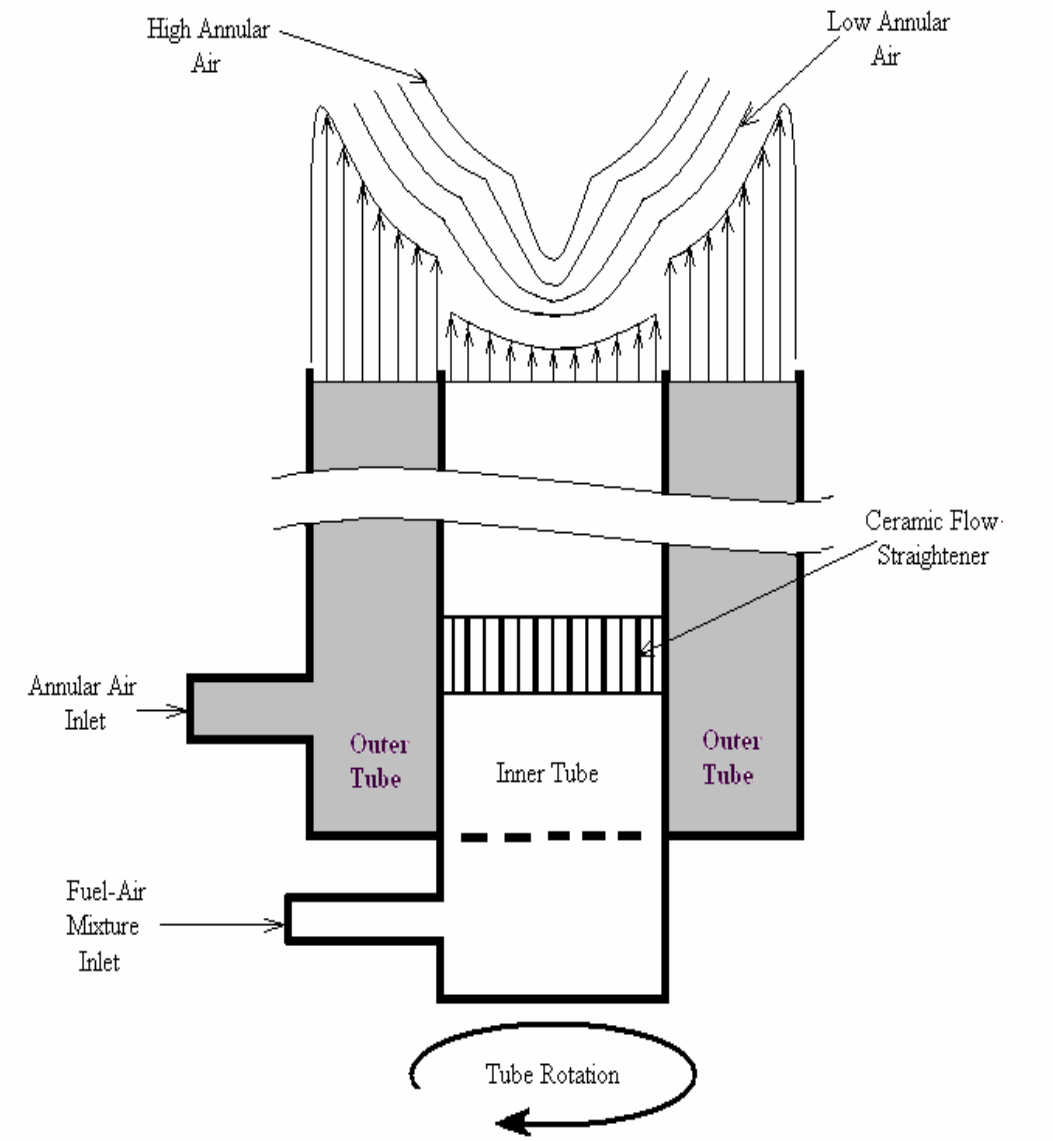

Figure 3.1.18: Schematic diagram of fuel-air flow velocity with annular airflow subjected to the rotation of inner burner tube.

Further increase of annular air to 142 cm/s (shown in Figure 3.1.17) causes the flame to mix and rotate even more until a “Pinching Flame” appears. The flame looks brighter and spins with a tail looking appearance at its bottom.

3.1.4 Flame stability limit

3.1.4.1 Blowoff event

Blowoff of lean premixed flames by increasing flow velocity for mixture of equivalence ratio is kept at 0.46 and rotational speed at 2760 rpm are shown in Figure 3.1.19. Figure 3.1.19 (a) shows a nonrotating lean flame with mixture equivalence ratio of 0.46 and initial flow velocity of 213 cm/s. The lean flame is long, steady, blue in color with a near white boundary or surface. At the start of the rotation flame starts to look unstable with a wavy cone shape (Figure 3.1.19 b). Centrifugal force due to rotation causes this tall flame to shake sideways and the flame apparently reduces in height. The rotation also causes the flame base to detach from the burner rim tightly cause the destabilization of the whole flame. Keeping the flow velocity and rotational speed fixed, the flame remains in the dancing state without blowing off. In this particular condition the flame speed and flow velocity balance each other, thus keeping the flame on top of the nozzle. But as soon as the flow velocity increases to 240 cm/s, drastic change happens. The flame in Figure 3.1.19 (c) looks very unstable and finally blows off. Without rotation an increase in flow velocity only increases the flame height. With rotation, an increase in the flow velocity adds to the instability of the flame where the addition in flame height, subjected to centrifugal force causes the flame to wiggle beyond the equilibrium balance between the flame speed and flow velocity, thus blows the flame away from the burner rim.

Blowoff can also occur by increasing annular air on nonrotating-premixed flame. As shown in Figure 3.1.20 (a), without annular air and tube rotation high flow velocity (214 cm/s) of fuel-lean (ϕ = 0.6) premixed flames naturally look long and thin. Introduction of the annular air gives some effect on the flame stability. In Figure 3.1.20 (a) the flame color is whitish blue and it attaches steadily on top of the burner rim. Annular air reduces the temperature of the burner tube. This can become a stabilizing factor because the colder rim makes a better heat sink for the attachment of the flame.

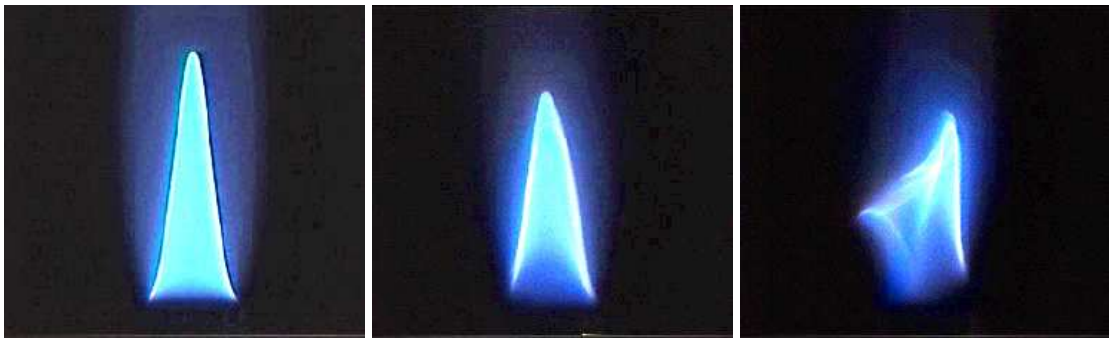

(a) (b) (c)

Figure 3.1.19: The effect of increasing the flow velocity on rotating lean premixed flame: $\phi = 0.46$,

(a) Nonrotating, (b) Rotating with $\omega = 2760$ rpm, V = 213 cm/s,

(c) Rotating with $\omega = 2760$ rpm, V = 240 cm/s.

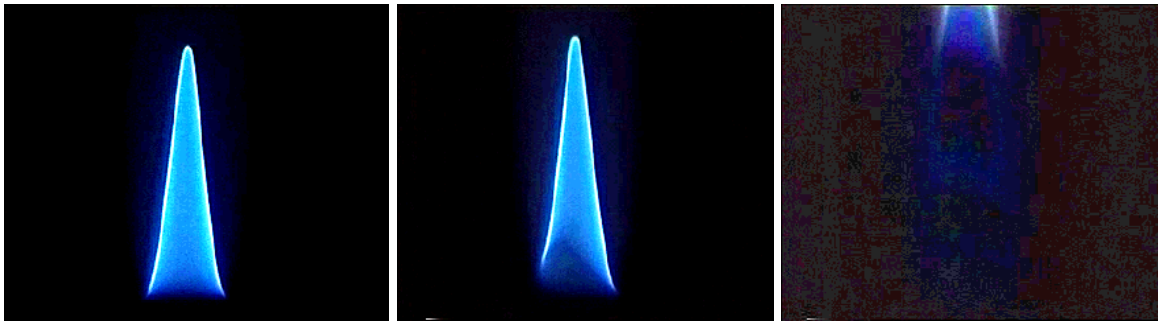

(a) (b) (c)

Figure 3.1.20: The effect of increasing annular air on nonrotating premixed flame.
ϕ = 0.6, V = 214 cm/s and without rotation.
(a) V_{aa} = 36 cm/s, (b) V_{aa} = 64 cm/s, (c) V_{aa} = 75 cm/s.

Annular air supplies more aeration to the flame and this might cause the equivalence ratio of the mixture to decrease and reduce the flame speed. This also explains the long and thin flame shown in Figure 3.1.20 (a). As the velocity of the annular air increases, a point comes when the speed of the flame keeps on decreasing until it does not match the mixture velocity flowing upward. Also the forward thrust of the air causes the flame to be unstable and as the velocity reaches 64 cm/s (shown in Figure 3.1.20 (b)) the base of the flame starts to be lifted few centimeters from the rim. Further increase of the annular air finally causes the flame to be blown completely away from the burner rim (shown in Figure 3.1.20(c)).

The effect of increasing annular air on rotating lean premixed flame that leads to blowoff is shown in Figure 3.1.21. The flame in Figure 3.1.21 is the same as flame shown in Figure 3.1.20 but here the burner is rotating at the speed of 2760 rpm. The rotation normally causes the tip buckling in low and average mixture velocity flows. But burner rotation on high velocity flows will not buckle the flame but rather will shake the flame cone especially when the annular air is applied. This is shown in Figure 3.1.20 (a).

Increasing annular air from 43 cm/s to 53 cm/s causes the flame to shake vibrantly. Rotation causes the flame base not to be able to attach on the burner rim firmly. Moreover the application of annular air increases local air mixing, reduces the mixture equivalence ratio and hence reduces the local flame speed. In certain cases if too much mixing occurs, local quenching can occur and hence causes the overall flame not to be able to cling on the rim. The application of annular air that is acting upward will cause the flame base at the moment it is not attaching on the rim to be blown upward. This happens intermittently causing the flame to look like having several layer of thin flame dancing on top of the burner rim. Increasing annular air to 68 cm/s finally causes the flame to be blown away from the burner rim. As expected, this happens at a

lower annular air velocity compared to its nonrotating counterpart (75 cm/s) such as shown in Figure 3.1.21 (c).

(a) (b) (c)

Figure 3.1.21: The effect of increasing annular air on rotating premixed flame,
Premixed flame of propane: $\phi = 0.6$, V = 214 cm/s, $\omega = 2760$ rpm
(a) $V_{aa} = 43$ cm/s, (b) $V_{aa} = 53$ cm/s, (c) $V_{aa} = 68$ cm/s.

Figure 3.1.22 shows the events of flame liftoff on rich-fuel mixture ($\phi = 2.87$) with a low flow velocity (V = 31.7 cm/s) and burner rotational speed of 2760 rpm. The rich flame is shown to have two distinct luminous regions, blue in the bottom and sooty orange flame on the top part. By increasing the annular air, the rotating flame shows dramatic changes in its appearance. Starting with annular air of 67.5 cm/s the flame shows slight disturbances where the flame is waving from side to side. There are two factors involved in influencing the behaviors of the flame in that condition. One is burner rotation and the other is the application of annular air. Introduction of annular air increases the mixing process. In this experiment, friction between inner tube and flowing annular air causes the annular air to swirl. Swirling motion of the annular air causes the flame that sitting on the rotating burner to wave from side to side. Rigorous mixing is expected as the velocity of the annular air increases from 67.5 cm/s to 74.6

cm/s. This could be seen by the reduction of the sooty orange flame on the upper section of Figure 3.1.22(b). Enhanced mixing especially in the most bottom section of the flame to get leaner thus reduces the local flame speed. The increasing swirling motion of the annular air also causes some parts of the flame to get lifted from the rim. This explains the intermittent lifting of the flame base from its burner rim. Centrifugal force acting on the flame also causes the flame to offshoot from its main body. As the annular air increases to 83.5 cm/s, the stronger swirling motion causes flame to be lifted totally from the burner rim (Figure 3.1.22 c). The enhanced mixing also causes the sooty yellow flame to get smaller and in this figure, Figure 3.1.22 (c), only small traces are left at the upper part of the flame.

(a) (b) (c)

Figure 3.1.22: Liftoff event of rotating premixed gas under increasing annular air in a rich premixed gas case: $\phi = 2.87$, V = 31.7 cm/s, $\omega = 2760$ rpm
(a) $V_{aa} = 67.5$ cm/s, (b) $V_{aa} = 74.6$ cm/s, (c) $V_{aa} = 83.5$ cm/s.

(a) (b) (c)

Figure 3.1.23: Liftoff event of rotating premixed gas under increasing annular air in a very rich premixed gas case: ϕ = 4.31, V = 33.4 cm/s, ω = 2760 rpm (a) V_{aa} = 36 cm/s, (b) V_{aa} = 64 cm/s, (c) V_{aa} = 114 cm/s.

The flames in Figure 3.1.23 are almost the same as the flame in Figure 3.1.22 but here the flame is richer (ϕ = 4.31). Richer mixture is shown to require a higher annular air velocity (in this case, annular air of 114 cm/s) to lift up the flame from its burner rim. The lifted flame is shown to be more dynamic with totally blue color, indicating good mixing.

The basic effect of increasing annular air on stationary premixed flame is shown in Figure 3.1.24. Flame condition in Figure 3.1.24 is the same as in Figure 3.1.22 except that the burner is not rotating. As a result the flame is shown to be lifted only at higher annular air flow velocity of 135 cm/s compared to 83.5 cm/s in the rotating case of Figure 4). Starting with annular air of 117 cm/s the flame is shown to be attached on its burner rim. As soon as the annular air increases to 120 cm/s some part of the flame is seen to lift from the rim. The flame is completely lifted off from the rim once the annular air is increased to 135 cm/s.

In Figure 3.1.25 the flame is fuel-lean (ϕ = 0.72) and the mixture flow velocity is small (V = 29.1 cm/s). The annular air flows at constant, high velocity of 142 cm/s. Without rotation (Figure 3.1.25 a) the flame is having dual cone; inner and outer cones. At a rotational speed of 3240 rpm, flame completely lifts off from the burner rim and forms a “Pinching Flame”. Burner rotation causes the annular air to swirl. Swirling

motion of the annular air rotates the whole flame. Rotation of the flame increases the fuel-air mixing, reduces the equivalence ratio and hence reduces the flame speed. The reduction of the flame speed causes it to find a new equilibrium position, where the flame speed and flow velocity matches.

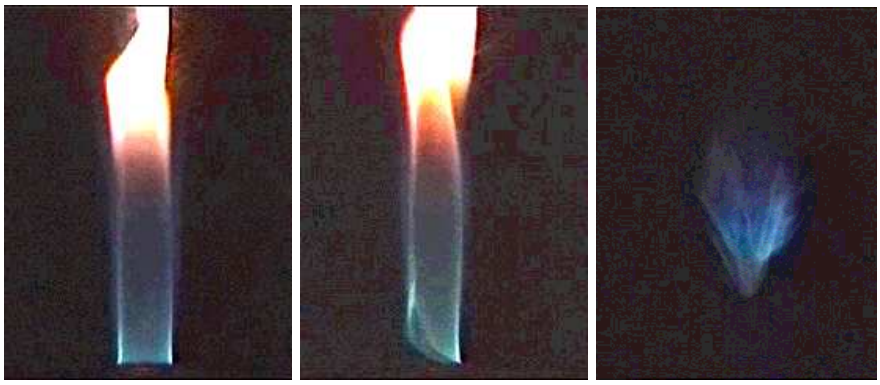

(a) (b) (c)

Figure 3.1.24: Liftoff event of nonrotating rich premixed gas under increasing coaxial air. Premixed propane gas: ϕ = 2.87, V = 31.7 cm/s, Re = 487. Without rotation
(a) 117 cm/s, (b) 120 cm/s, (c) 135 cm/s.

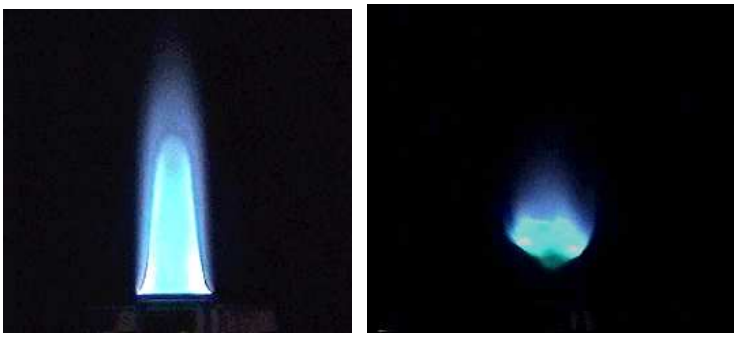

(a) (b)

Figure 3.1.25: The effect of rotation on premixed flame with annular air applied. Mixture ϕ = 0.72, V = 29.1 cm/s
(a) No rotation, (b) ω = 3240 rpm.

(a) (b) (c)

Figure 3.1.26: The effect of increasing annular air on lean premixed flames. ϕ = 0.32, V = 109 cm/s, Re = 1678. Burner rotational speed = 3240 rpm
(a) No annular air, (b) V_{aa}= 46 cm/s, (c) V_{aa} = 78 cm/s.

The effect of increasing annular air on rotating premixed flame is shown in Figure 3.1.26. The flame mixture is very lean (ϕ = 0.32) and the flow velocity is moderate (V = 109 cm/s). The flame initially (Figure 3.1.26 a) looks steady with a single sharp cone appearance. This blue flame has a bright whitish boundary. As the air is introduced (V_{aa} = 46 cm/s), the flame starts to shake vigorously and as soon as the annular air increases to 78 cm/s (Figure 3.1.26 c), the flame blows off from the burner rim.

3.2 Premixed flame height

Flame height is one of the important parameters in flame investigation. In this section we consider the effect of burner rotational speed, equivalence ratio and nozzle geometry on the flame height. The following discussion is divided into three parts. In the first part we discussed about the flame height from circular nozzle burner. Then the discussion will be followed by the measurement of flame height from burner of different nozzle geometry, such as oval, triangular, and rectangular.

3.2.1 Circular nozzle burner

Figure 3.2.1 (1) shows the variation of the flame height as a function of mixture equivalence ratio at burner rotational speed of 3240 rpm and 4500 rpm. The mixtures exit velocity is 94 cm/s the equivalence ratio of the mixture is ranging from 0.42 to 1.06. As the equivalence ratio increases, the velocity also increases from 92.5 cm/s to 95.2 cm/s. For the nonrotating burner, the flame height shows little increment for the equivalence ratio from 0.4 to 0.6. But as soon as the equivalence ratio increases to the value beyond 0.6 the flame height increases drastically until the flame height reaches its maximum value about 7.2 burner diameters and this occurs at equivalence ratio of 1.08, slightly on the richer side or greater than stoichiometry.

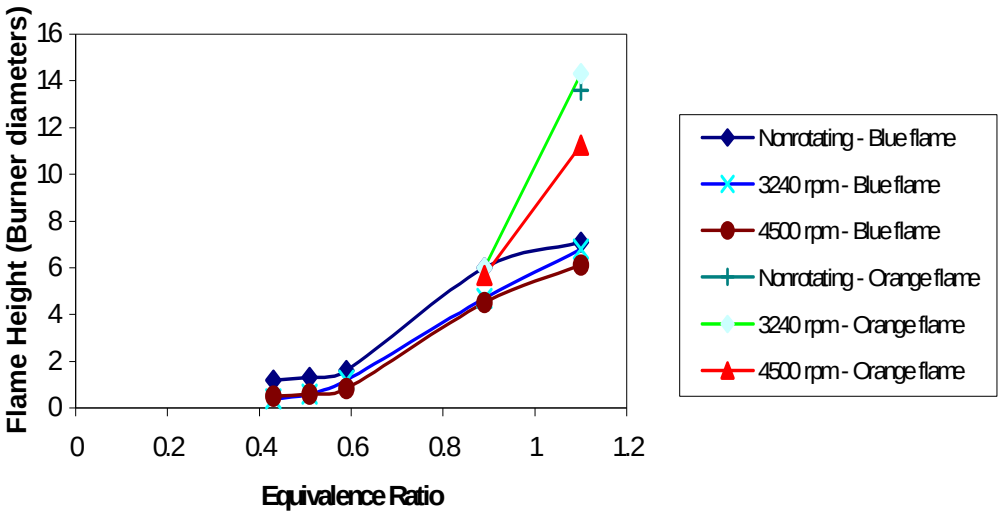

Figure 3.2.1: Effect of burner rotational speed on flame height. Flame height versus equivalence ratio at different burner rotational speed. V = 94 cm/s

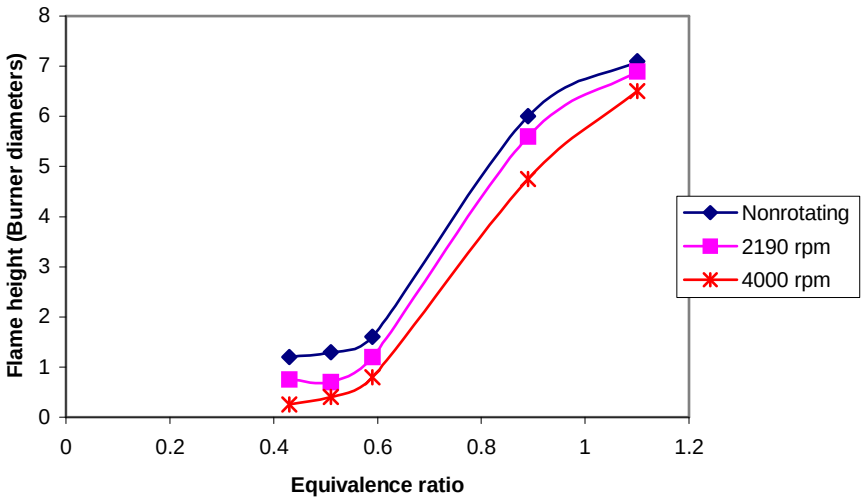

Figure 3.2.2: Effect of burner rotational speed on flame height. Flame height versus equivalence ratio at different burner rotational speed.

As shown in Figure 3.2.2, the flame speed varies with equivalence ratio. In general the flame speed is maximum at stoichiometry. So for the nonrotating burner discussed earlier, as the equivalence ratio increases to unity, the flame speed increases and as the mixture velocity remain constant the flame is subsequently reduces in height. The flame color is blue for equivalence ratio below unity but as the equivalence ratio reaches unity orange color flame at the top part start to appear.

As the burner rotated with the rotational speed of 3240 rpm the flame height at fixed equivalence ratio reduces. As the rotational speed increases to 4500 rpm, the flame height is further reduces only slightly. Rotational effect, which mainly affects the bottom of the flame, increases the mixing process thus gradually turning the long luminous orange flame into a shorter bluish one.

The effect of rotation and equivalence ratio on the height of the blue flame is shown much clearer in Figure 3.2.3 and Figure 3.2.4. In Figure 3.2.3 the mixture velocity is fixed at 94 cm/s and the equivalence ratio is decreases from 1.56 to 0.89. In nonrotating

case as the equivalence ratio decreases from 1.56 to 0.89, the flame height decreases to half of its original height, from 12 to 6 burner diameters.

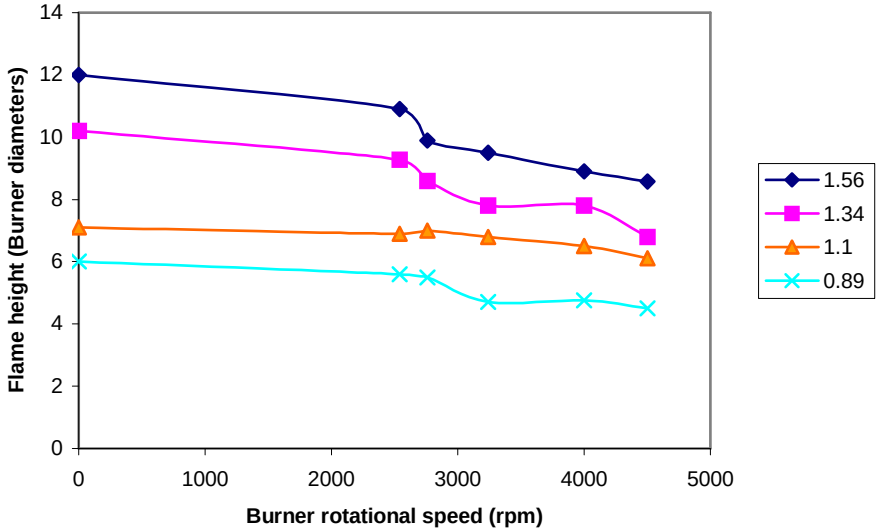

Figure 3.2.3: Flame height versus burner rotational speed for equivalence ratio of 0.51 to 1.56.

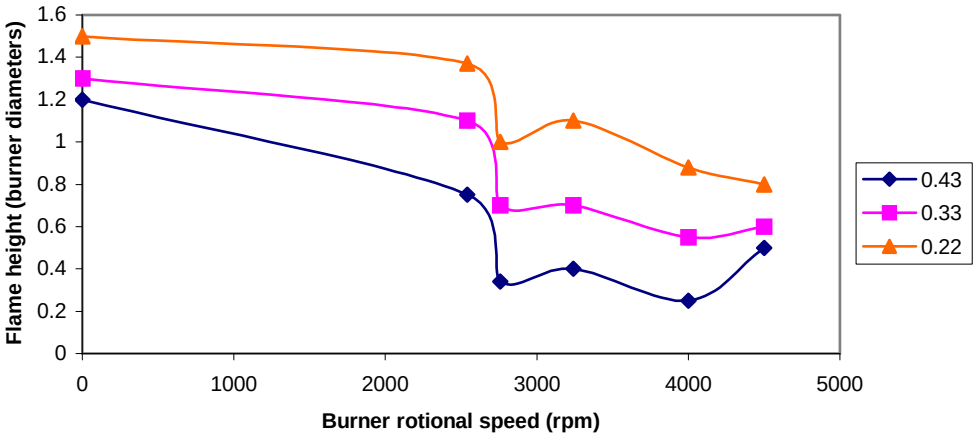

Figure 3.2.4: Blue flame height versus burner rotational speed at equivalence ratio of 0.22 to 0.43. Flame height versus burner rotational speed at equivalence ratio of 0.43, 0.33, 0.22 – V = 94 cm/s

However the rate of flame height reduction due to the increasing the tube rotational speed becomes smaller at lower mixture equivalence ratios. At constant rotational speed, as the equivalence ratio decreases to unity the flame speed also decreases (as depicted in Figure 3.2.2). As the mixture flow velocity is kept constant, the increasing flame speed causes the flame to get shorter.

A different behavior for the flame height is observed in Figure 3.2.4. For the stationary case as the equivalence ratio decreases from 0.43 to 0.22 the flame height increases from 1.2 to 1.5 burner diameters. According to Figure 3.2.2, in the lean side, the flame speed decreases as the equivalence ratio decreases from 0.43 to 0.22. At fixed mixture velocity, as the flame speed decreases, the flame height increases. The increment in flame height upon decreasing the mixture equivalence ratio is enhanced by the introduction of burner rotation. Burner rotation enhance fuel-air mixing, causes a lean mixture to getting leaner. This will further decrease the flame speed and hence increases the flame height. The increment in flame height by reducing the equivalence ratio from 0.43 to 0.22 is the largest for the rotational speed of 3200 rpm.

3.2.2 Burner of various nozzle geometries

The experiments of burner having several nozzle geometries have been conducted in order to see the difference of flame characteristics and stabilities compared to their circular nozzle counterpart. The following section described the results of the experiments. The effect of burner rotational speed on flame height at different values of equivalence ratio for circular and oval nozzles are shown in Figure 3.2.5 (a) and (b), respectively. The mixture equivalence ratio is varied from 0.5 to about 1.5.

For the case of nonrotating circular nozzle, such as shown in Figure 3.2.5 (a), an increase in equivalence ratio, causes the flame to increase in height, from 1.8D for ϕ of 0.5 to 12D for ϕ of 1.5. There is not much increased in the flame height for ϕ ranging from 0.5 to 0.9 but as soon as ϕ exceeds 0.9 there is a drastic increase in flame height until it reaches 12D for ϕ of 1.5.

As the burner of circular nozzle rotated at ω of 2190 rpm, the flame reduces in height. The reduction in height is shown to be in effect only for ϕ of 0.9 and beyond. At ϕ of 1.5, the flame height is about 7.5D. As the rotational speed increases to 3240 rpm, further reduction in flame height is noticed. Again it occurs only for ϕ of 0.9 and higher. It is observed that at 3240 rpm, the flame remains at the same height (which is at about 4.2D) for ϕ of 1.2 and higher.

(a)

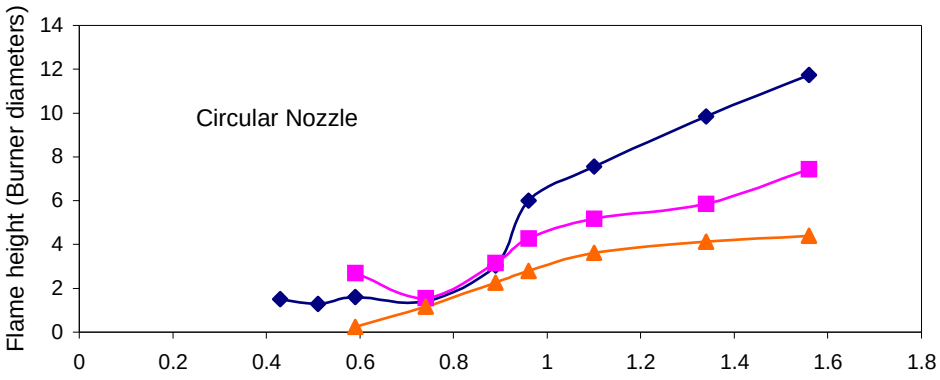

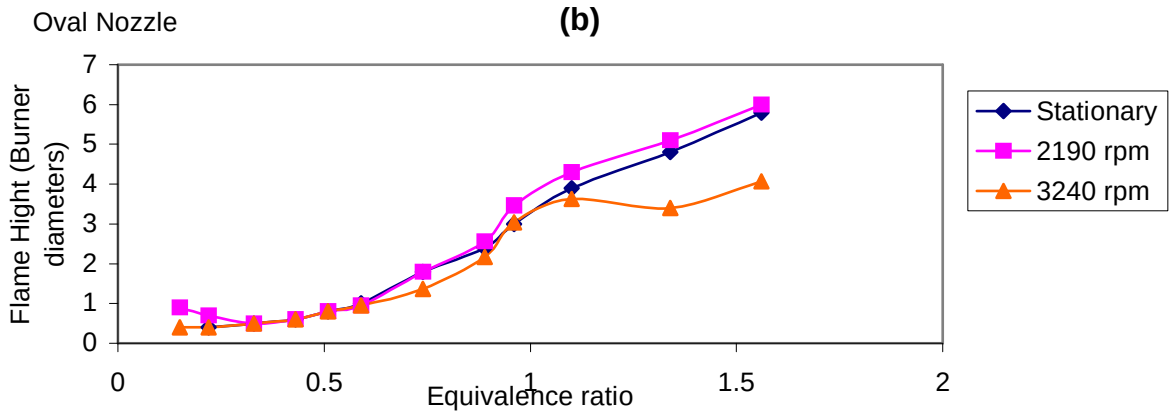

Figure 3.2.5: Flame height versus equivalence ratio of circular and oval nozzle burner at burner rotational speed of 0, 2190 and 3240 rpm.

For the case of nonrotating oval nozzle burner (Figure 3.2.5 b), the increment in flame height due to the increase in ϕ can be observed for almost the whole range of ϕ, starting from fuel-lean (ϕ of 0.2) to fuel-rich (ϕ of 1.5). The flame height of nonrotating oval nozzle burner at ϕ of 1.5 is about half of the flame height produced from the nonrotating circular nozzle burner. This shows how a dramatic decrease in flame height could be achieved by changing the shape of the burner nozzle, e.g., from circular to oval.

The Figure 3.2.5 (b) shows the effect of rotation on oval nozzle burner. When the inner burner tube rotates at two different rotational speeds, two types of results are observed. At the speed of 2190 rpm, flame height increases to about 0.4D. Even though the increment in height is not that significant, contrary to any other observation on other type of nozzles, oval nozzle burner rotating at 2190 rpm shows a different behavior. As the tube rotational speed increases to 3240 rpm the flame height drops to 4D. This happens only at ϕ ranging from 1.2 and higher. It is concluded that for the oval nozzle, the reduction of flame height can be achieved by rotating the tube fast enough, i.e. rotational speed beyond 3000 rpm. The effect of burner rotational speed on flame height

at different values of equivalence ratio for triangular and rectangular nozzle is shown in Figure 3.2.6 (a) and (b). In Figure 3.2.6 (a), nonrotating triangular nozzle producing a flame with the height of about 4.5D at stoichiometry and 8D at ϕ of 1.5. For the lean mixture, ranging from 0.5 to 1.0, rotating the inner tube of triangular nozzle does not cause much reduction in the flame height. The flame height starts to reduce quite significantly for the fuel rich mixture (ϕ of 1.0 and above). The flame height reduces for almost 2D for the equivalence ratio of 1.5. Increasing the rotational speed to 3240 rpm causes the height of flame to further reduced for another 1D at ϕ of 1.5.

The behavior of the flame height shown by the triangular nozzle burner (Figure 3.2.6 a) is reflected in its rectangular nozzle counterpart, shown in Figure 3.2.6 (b). The only difference is that as the rotation starts, the flame height reduces uniformly at about 1D throughout for the ϕ ranging from 1.0 to 1.5.

(a)

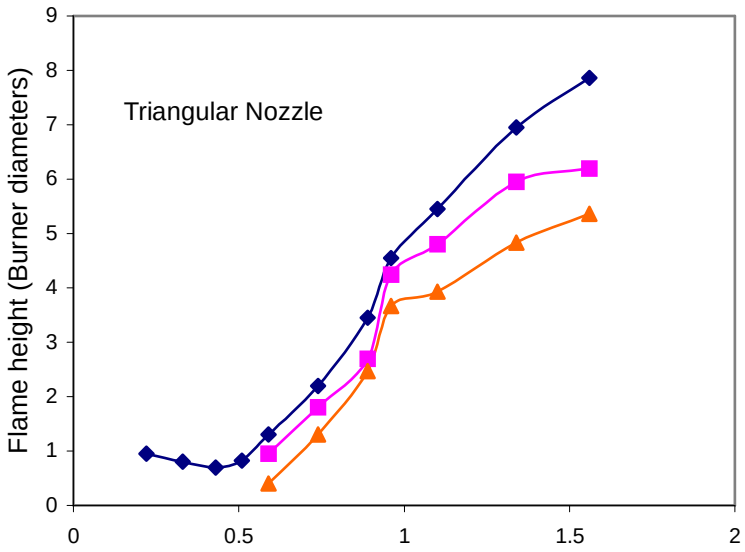

(b)

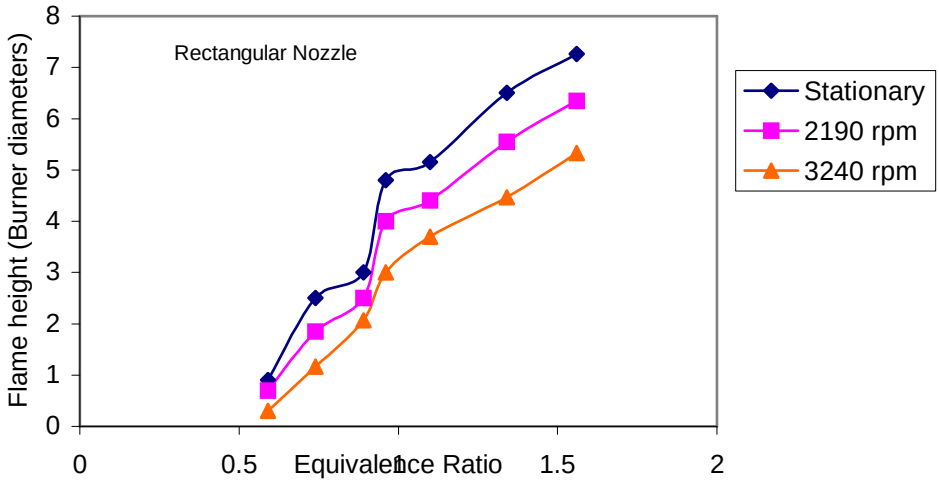

Figure 3.2.6: Flame height versus equivalence ratio of triangular and rectangular nozzle burner at burner rotational speed of 0, 2190 and 3240 rpm.

A much clearer comparison of flame height produced from the burner of different nozzle geometries (circular, oval, triangular and rectangular nozzle) at three different rotational speeds 0, 2190 and 3240 rpm is shown in Figures 3.2.7 (a), (b) and (c) respectively. For the nonrotating case, such as shown in Figure 3.2.7 (a), at stoichiometric mixture ($\phi = 1$) the circular nozzle burner produces the tallest flame (about 6.5D) whereas the oval nozzle burner produces the lowest (about 3.2D). Triangular and rectangular nozzle produces flame of about 5D tall at stoichiometry. This reiterates the discussion of Figure 3.2.5 that in nonrotating case, burner geometry plays major affect in the flame height.

As shown in Figure 3.2.7 (b) and (c), burner rotation causes the height of flame produced by four different nozzles to merge. For rotational speed of 2190 rpm and

at stoichiometry mixture, the flame of every nozzle geometry merges to the average height of 4D. For burner rotating at the speed of 3240 rpm (Figure 3.2.7 b) the flame merges to the height of 3.5D at $\phi = 1$. These observations show that for rotating case, the burner rotational speed plays much more important role compared to nozzle geometry in changing the height of the flame.

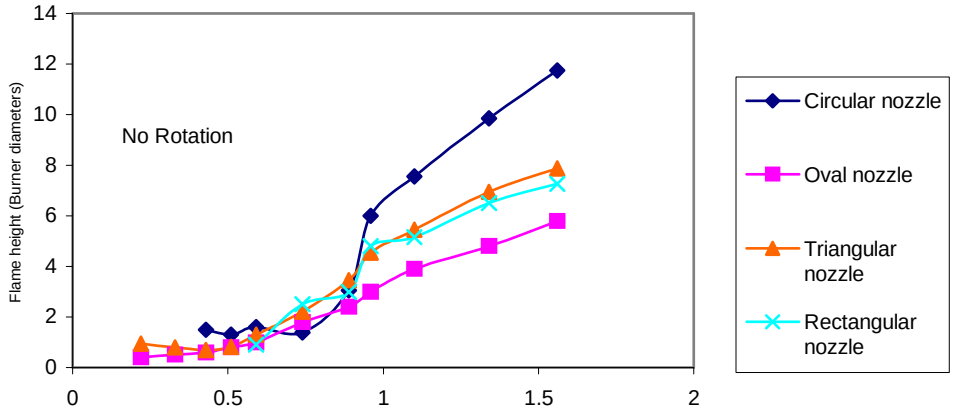

(a)

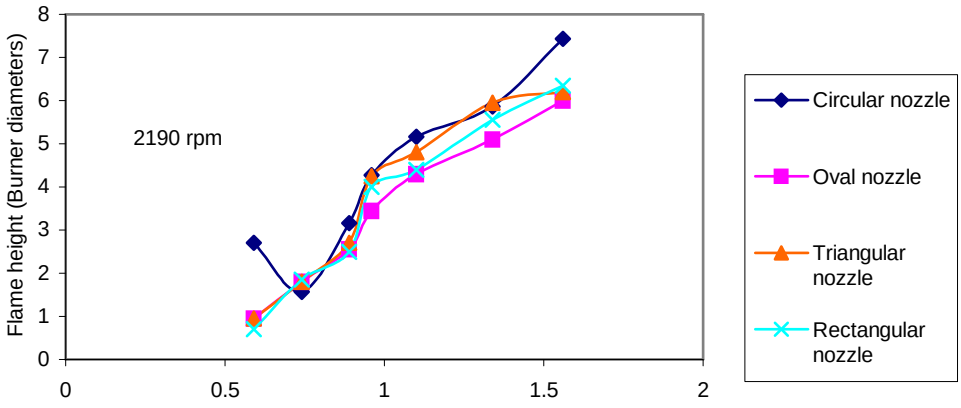

(b)

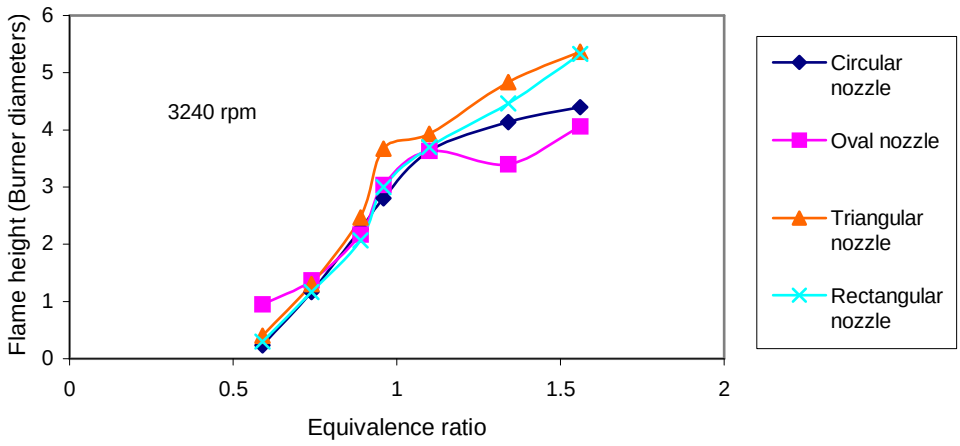

(c)

Figure 3.2.7: Flame height versus equivalence ratio for various nozzle geometries at burner rotational speed of 0, 2190 and 3240 rpm.

Figure 3.2.8 shows the effect of burner rotational speed at different equivalence ratios. For circular nozzle, shown in Figure 3.2.8 (a), mixture of ϕ = 1.5 the flame height decreases from 12D at stationary to 5D at 3200 rpm whereas for ϕ = 0.59 the flame does not decreasing but in fact increases very slightly. The increment in the flame height with rotational speed is shown clearly for lean mixture of ϕ = 0.74. At ϕ = 1.5, the flame is fuel-rich. For fuel-rich mixture, the increase in rotational speed will enhance mixing. Higher degree of mixing reduces the equivalence ratio and hence increases the flame speed. As the mixture velocity is fixed, the increase in flame speed will shorten the flame height. At ϕ = 0.74, the flame is fuel-lean. As discussed earlier, the increase of rotational speed enhances mixing. This makes the fuel-lean much leaner, thus decreases the flame speed. As the mixture velocity is fixed at 94 cm/s, the decrease in flame speed increases the flame height.

(a)

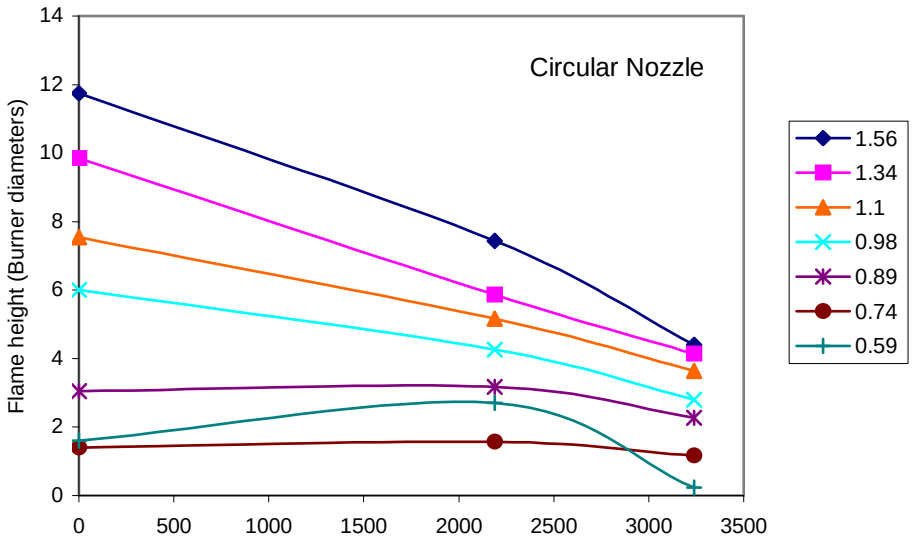

(b)

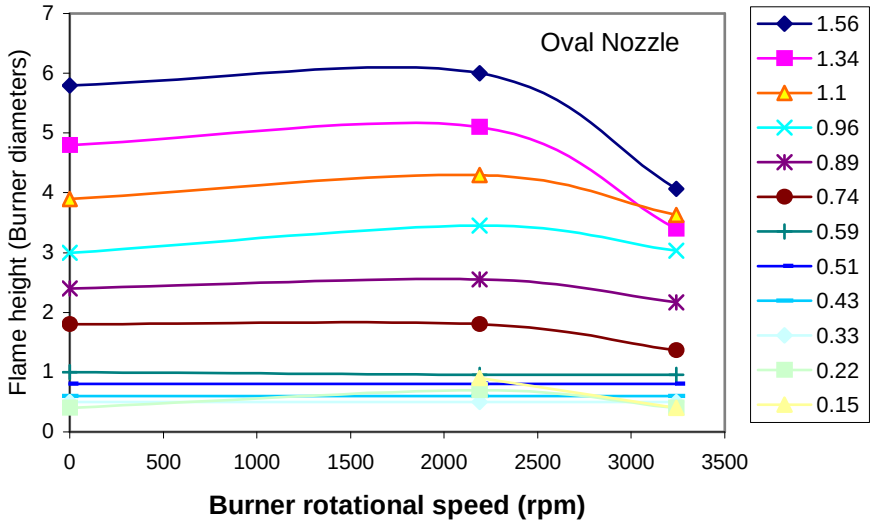

Figure 3.2.8: Flame height versus burner rotational speed for circular and oval nozzle burner at various mixtures equivalence ratio.

(a)

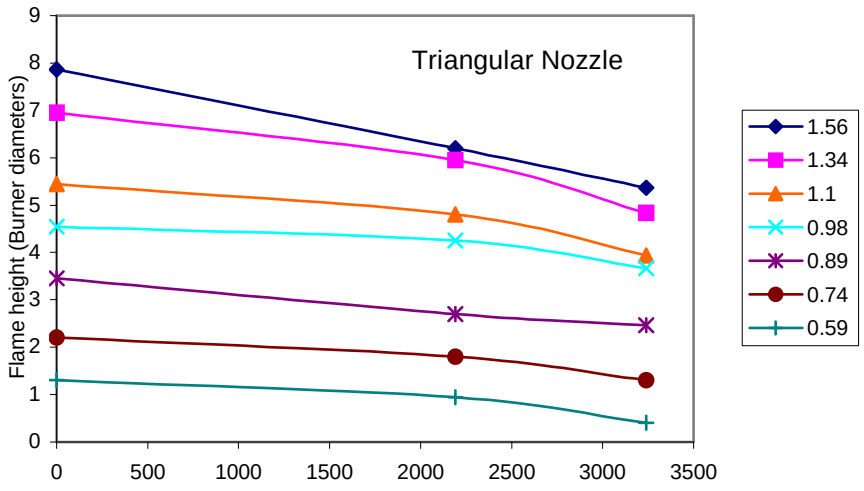

(b)

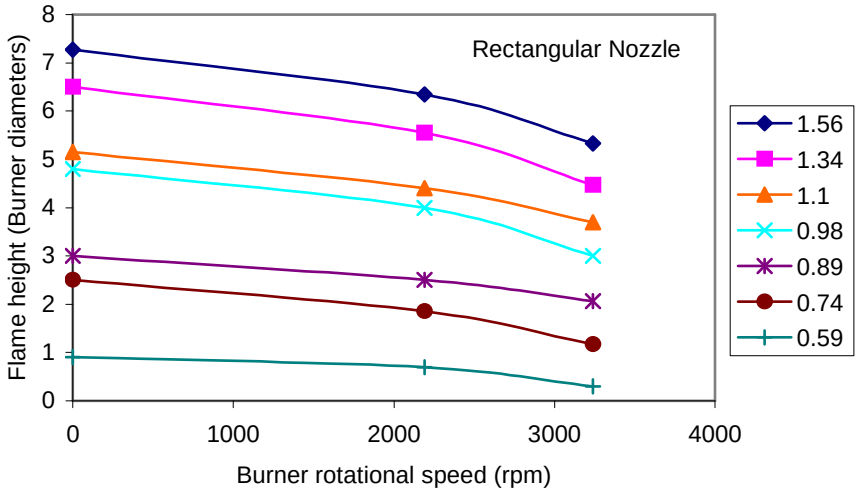

Figure 3.2.9: Flame height versus burner rotational speed for triangular and rectangular nozzle burner at various mixtures equivalence ratio.

Similar discussion is applied on the flame produced by the burner of different geometries such as triangular and rectangular nozzles, as shown in Figure 3.2.9 (a) and (b). The only difference is that the height of flame for triangular nozzle burner with ϕ of 1.56 reduces from 8D for nonrotating case to 5.8D for ω = 3200 rpm, whereas for rectangular nozzle burner the flame height reduces from 7.2D for ω = 0 to 6D for ω = 3200 rpm. However, for oval nozzle burner a different behavior is observed. As shown in Figure 3.2.8 (b), for ϕ of 1.56 to 0.96, as the rotational speed increases from zero to 2000 rpm, the flame increases in height. But further increase in rotational speed to 3500 rpm, reduces the flame height.

Figure 3.2.10 illustrates the effect of rotation on the flame height for mixtures of fixed equivalence ratio and for burner of different nozzle geometries. The burner rotates at different speed with the fuel-air mixture flows at fixed velocity of 94 cm/s. It is observed that circular nozzle burner produces the tallest flame and this is true for almost the whole range of mixtures equivalence ratio. The use of nozzles other than circular (such as triangular, rectangular and oval) shows beneficial to the overall reduction of the flame height. This is true even for the nonrotating case. The difference in the flame height for various nozzle geometries is shown to be the largest for the rich mixture (ϕ = 1.56 of Figure 3.2.10a) and the smallest for the lean mixture (ϕ = 0.59 of Figure 3.2.10c). As discussed earlier, the flame height decreases for burner of different geometries. In general, the flame height decreases by using nozzles in the following order: circular, triangular, rectangular and oval. The introduction of rotation causes the flame to get shorter in height. The flame height reduces with rotational speeds until they merge. Although the flame height merges to a different point for every equivalence ratio, all of them occurred at the rotational speed of 3200 rpm. This behavior is repeated for ϕ of 0.96, but not for the flame from oval nozzle burner at ϕ = 0.59. For the oval

nozzle burner, the flame height at ϕ = 0.59 does not change with respect to the increasing burner rotational speed.

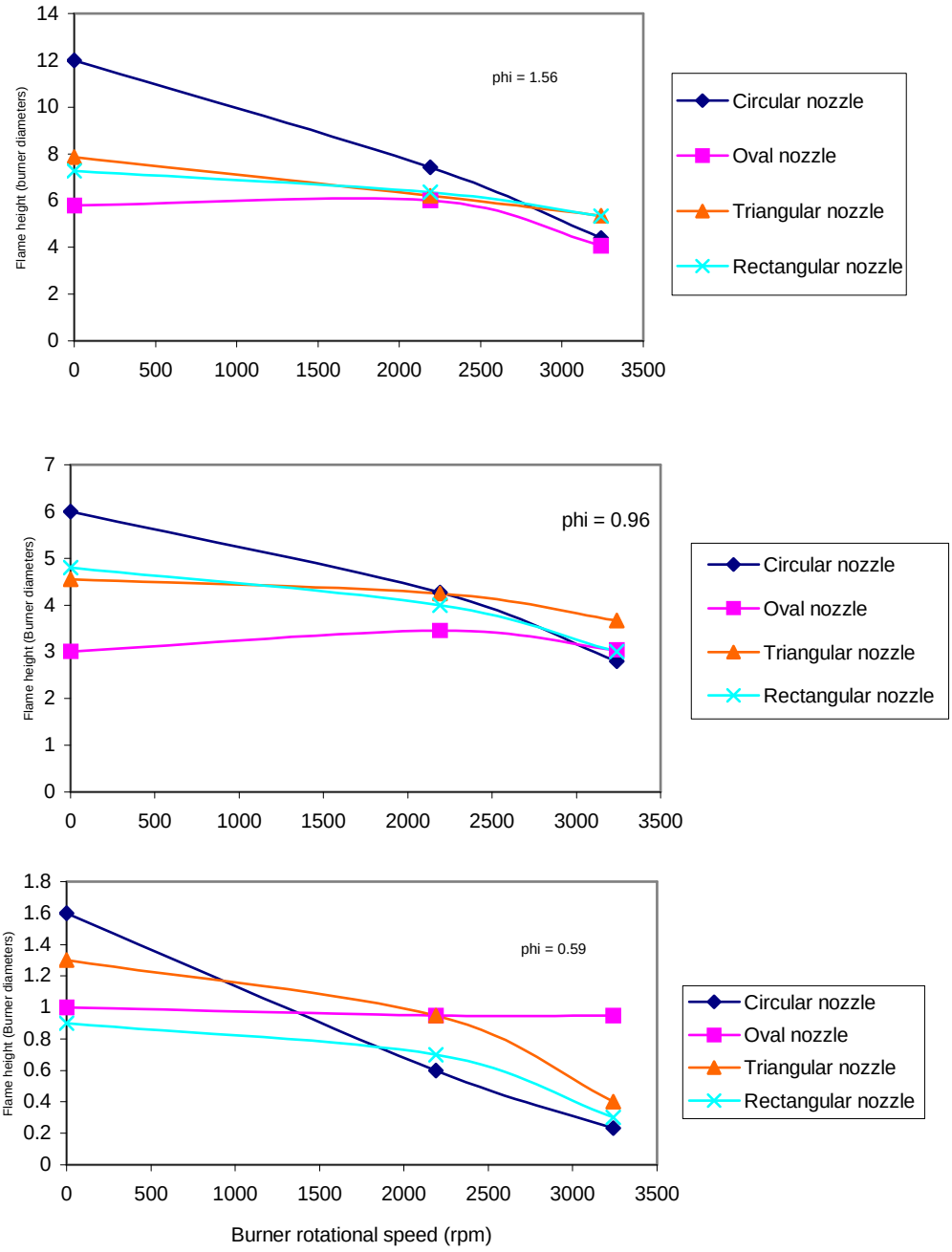

Figure 3.2.10: Flame height versus burner rotational speed at equivalence ratio of 1.56, 0.96 and 0.59 for various nozzle geometries.

Chapter 4

NONPREMIXED FLAMES

4.1 Introduction

This chapter deals mainly with the characteristics of the rotating nonpremixed flames from the double annular burner. In this study, we have considered the effect of several parameters on the characteristics of nonpremixed flame such as its shape, color, stability and height. The parameters considered are: rotational speed of the internal tube, fuel velocity, annular air and nozzle geometry. In the combustion literature, nonpremixed and diffusion terms are used interchangeably. In this dissertation, the name nonpremixed is most commonly used. The discussion about the nonpremixed flame in this chapter is divided into three parts. In the first part we discuss the effects of rotation and fuel velocity on the shape and the color of nonpremixed flames. In the second part, stability of nonpremixed flames will be discussed. Then the effect of nozzle geometries, fuel velocity, rotational speed and annular air on the flame height will be presented.

4.2 Nonpremixed flame characteristics

4.2.1 Effect of rotation on low velocity nonpremixed flames

Most of the flames considered in this section have low flow velocities. Figure 4.1 shows a typical small-nonpremixed propane flame stabilized on top of circular-nozzle burner. This type of nonpremixed flame has a very low exit velocity, about 0.2 cm/s. As observed in the picture, this simple nonpremixed flame of propane in the surrounding air is showing two distinct regions: the lower blue flame and an upper luminous orange flame. The region of luminous orange flame is due to emission by incandescent carbon particles. In the upper region of the vertical flame, there is sufficient quantity of hot gases that buoyant forces become important. Buoyancy accelerates the flow and causes a narrowing of the flame, since conservation of mass requires streamlines to come closer together as the velocity increases.

Figure 4.1: A low velocity stationary nonpremixed flame. V = 0.2 cm/s, $\omega = 0$

(a) (b) (c)

Figure 4.2: The effect of rotation on nonpremixed flames: V = 0.2 cm/s, ω = 2670 rpm.

Figure 4.2 shows the effect of burner rotation from early start of rotation to a steady state condition. This represent the flame for a speed of 2670 rpm having a velocity of 0.2 cm/s. Figure 4.2(a) shows that a slender flame suddenly changes to a round and short looking flame. This is due to centrifugal force that is acting outward thus widening the blue region of the flame. Figure 4.2 (a) is just shortly after the rotation is initiated. It therefore, represents, a very small rotation. Figure 4.2(b) represents the flame shape few seconds after the initiation of the rotation. And Figure 4.2(c) shows the flame after the establishment of a steady state rotating flame.

Initially a relatively large orange tip emerges. Rotation causes the velocity of the flow central section to slow down and consequently causes the central flow profile to buckle. This phenomena is shown clearly in Figure 4.2 (a) and (b) where the orange flame that is originally covering most of the upper part of the diffusion flame (such as depicted in Figure 4.1) is shown to get sucked toward the center of the burner rim and as this causes a soot wing to stick out of the orange flame tip. This penetration of soot is seen as a double, sticking upward orange flame located near the center of the semi hemispherical bluish flame. Rotation gradually makes the orange tip to become smaller. Finally, as shown in Figure 4.2 (c), the orange tip disappears. The flame then becomes

totally blue in color with tendency to curve down. Here the flame looks very interesting with a mushroom shape. It appears that the flame starts to float like a blue mushroom and have a tendency to buckle towards the center of rotation. The alteration of velocity profile due to rotation is shown schematically in Figure 4.3.

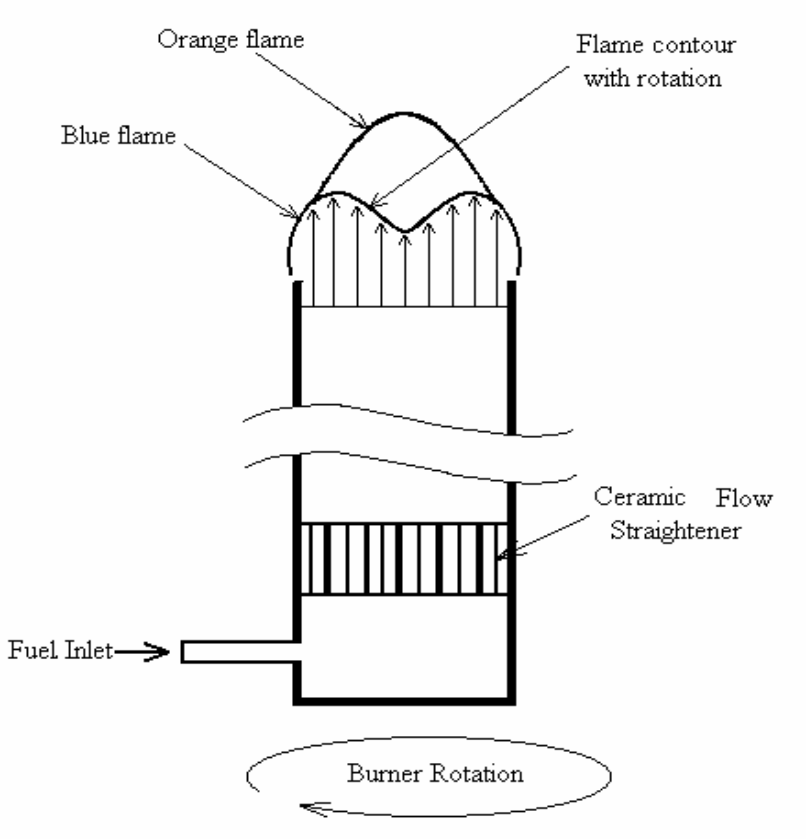

Figure 4.3: Schematic diagram of low flow velocity subjected to the rotation of burner inner tube.

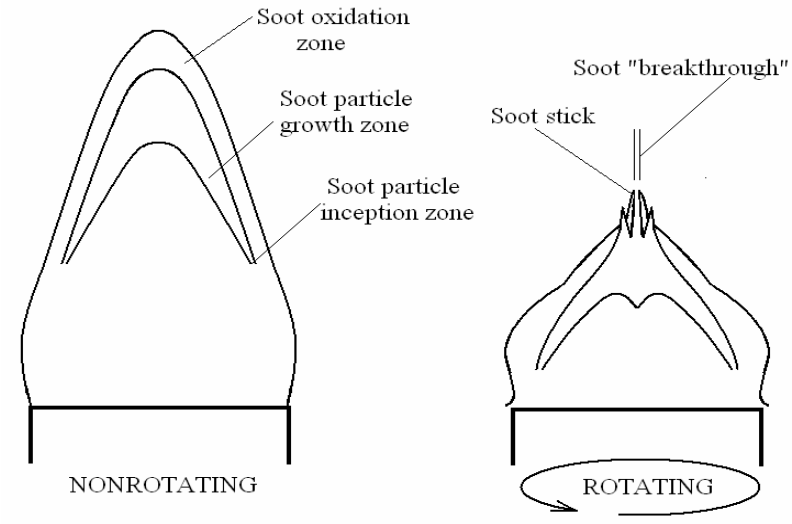

Figure 4.4: The formation of soot “wings” due to rotation.

The schematic diagram shown in Figure 4.4 helps to describe the formation of soot wing. As depicted in the diagram, rotation shortens the flame. When the flame gets shorter, soot has a shorter time to travel upward, going through the hot oxidation zone. As soot residence time gets shorter, all of the soot that is formed may not be oxidized on its journey through the high-temperature oxidizing region causing the appearance of soot “wings”. This soot “wings” is the soot that breaks through the flame and is normally referred to as smoke [16].

Figure 4.5 shows the effect of rotation on the nonpremixed flame, as the fuel flow velocity increases slightly to 0.83 cm/s. This low fuel velocity corresponds to Reynolds a number of 13. The flame shows two distinct regions; blue color at the lower section and orange flame at the upper section of the flame. The pictures show the gradual change of nonpremixed flames under the effect of burner rotational speed of 3240 rpm. In Figure 4.5(a), the burner is nonrotating and the diffusion flame shows blue flame at the bottom part and orange flame at the top part. In Figure 4.5(b), rotation started and this time the flame is shown to cling on the rim of the outer burner tube.

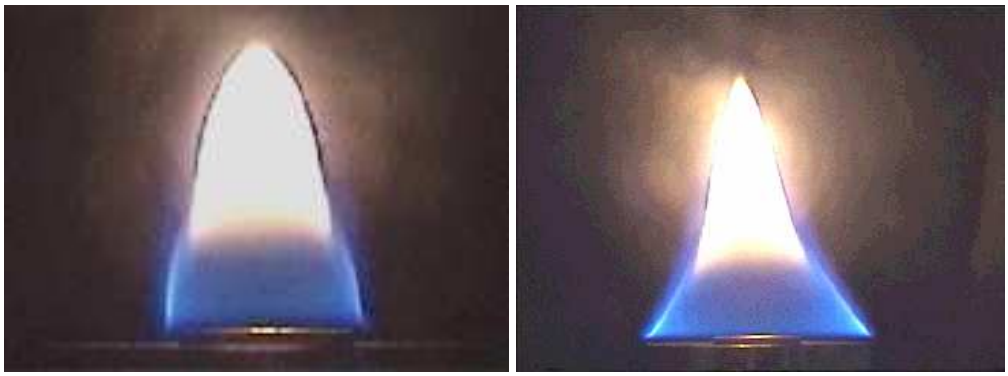

(a) No rotation (b) Rotating at the speed of 3240 rpm

Figure 4.5: Rotation effect of nonpremixed flame without coaxial air. Fuel velocity, V_f = 0.83 cm/s and Re = 13. Rotational speed, ω = 3240 rpm.

(a) (b) (c)

Figure 4.6: The effect of rotation on a very small nonpremixed flames, V = 0.83 cm/s. The sequence of pictures from (a) to (c) is the evolution of low velocity nonpremixed flames as the rotation of 3240 rpm starts.

The bottom blue section of the flame is shown to rotate steadily in the vicinity of the outer rim and it stays like that for the rest of its evolution. Similar to the nature of the lower velocity flame described in Figure 4.2, buckling of the center section of the flame causes the orange sooty region to be sucked inward, thus forming soot wings. The mixing process between the fuel and the air gradually turns the whole flame to bluish color flame, a sign of complete mixing. This time the mushroom like blue flame appears to be brighter as it rotates steadily on the burner port. Schematic diagram of the flame is shown in Figure 4.7

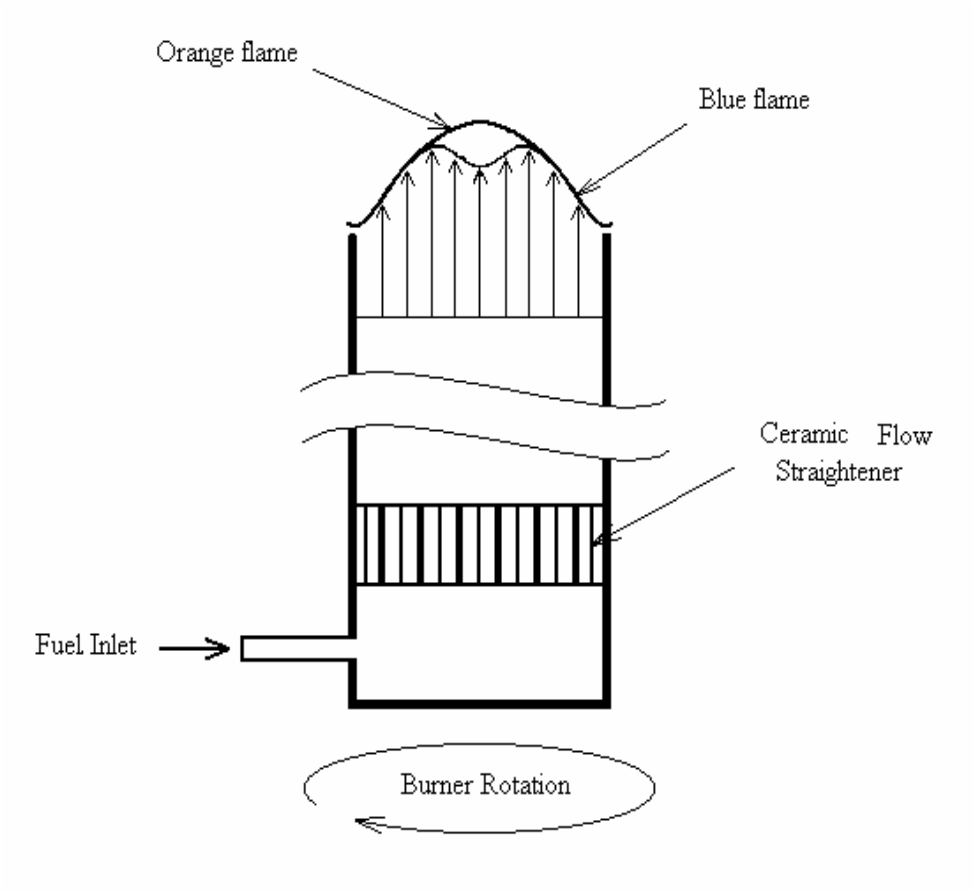

Figure 4.7: Schematic diagram of low flow velocity subjected to the rotation of burner inner tube.

Figure 4.8(a) shows a flame of higher fuel velocity without rotation. The flame looks taller than the one shown in Figures 4.1 and 4.5. This is obvious because in laminar flow region, the higher the fuel velocity the taller the flame. Burner rotational effect can be clearly seen in the rest of Figure 4.8. Especially from the slanted and top view such as shown in Figures 4.8 (c) and (d), respectively. It is observed that when the rotation starts, the central section of the mixture profile changes. As discussed earlier, rotation causes the blue section of the nonpremixed flame to buckle. Buckling elongates the middle orange region. It increases the orange flame region making it insufficient for the soot to be oxidized completely on its way out of the burner rim. As the rotation continues, fuel-air mixing increases as shown by the enlargement of blue flame region (Figure 4.8b) and flame gradually gets lower in height. When the rotating flame is viewed from an angle (slanting view) one can see the spiraling orange flame on top of the blue flame (Figure 4.8c). The flame is observed much better as it is viewed from the top (Figure 4.8d) where the spiraling orange flame is seen to rotate around a violet-blue circular flame. The top view clearly shows that rotation of the inner tube slows down the central flow velocity. This shifting-down action deprives the fuel from being exposed to the surrounding air. This in turn causes delays in central mixing and as a result orange flame seems to keep spiraling around the tube center.

(a)

(b) (c) (d)

Figure 4.8: Nonpremixed flame with fuel velocity fixed at 1.7 cm/s.
(a) Front view of nonrotating flame,
(b) Front view of nonpremixed flame rotating with speed of 2640 rpm,
(c) Slanted view of (b),
(d) Top view of (b).

4.3 Nonpremixed flame instability: Effect of rotation on nonpremixed flame with annular air applied.

Figure 4.9 shows interesting pictures of nonpremixed flame produced from the nonrotating double concentric burner. In this case, annular air is applied with flow velocity ranging from 85 cm/s to 142 cm/s. The flame appears initially as half blue and half orange (Figure 4.9a). As the annular air increases to 99 cm/s (Figure 4.9b), half of the flame bottom section starts to lift off from the burner rim. When the annular air reaches 120.8 cm/s (Figure 4.9c) the flame is completely lifted and dances vigorously about 1 cm above the burner rim. In this condition the flame is completely blue in color, showing well mixing. As the annular air increases further to 142 cm/s, a “pinching” flame appears. This type of flame is shaped like a blue torch with a trail at the bottom. These pictures show how annular air influence the appearance of the nonrotating, low velocity (0.83 cm/s) diffusion flame.

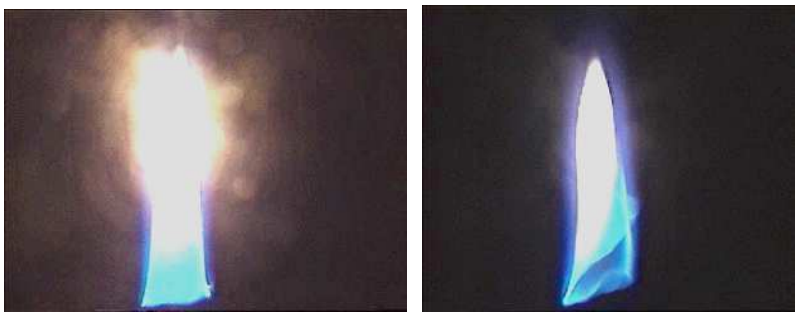

(a) (b)

(c) (d) (e)

Figure 4.9: Flame liftoff event for nonpremixed flames without burner rotation. Fuel velocity is constant at 0.83 cm/s.

(a) V_{aa} = 85 cm/s, (b) V_{aa} = 99 cm/s,

(c) V_{aa} = 120.8 cm/s, (c) V_{aa} = 129.3 cm/s,

(d) V_{aa} = 142.1 cm/s.

The effect of nonpremixed flame with fuel velocity of 6.3 cm/s and tube rotating at the speed of 2760 rpm is shown in Figure 4.10. At the beginning, Figure 4.10(a) shows all attached flame without rotation and without annular air. In Figure 4.10(b), there is still no rotation but annular air of 35.5 is applied. In Figure 4.10(c) a rotation of 2190 rpm and annular air velocity of 46.2 cm/s are applied. This immediately lifts the flame. In Figure 4.10(c), the rotation continues and as the annular air increases to 63.9 cm/s the flame immediately lifts off from the burner rim.

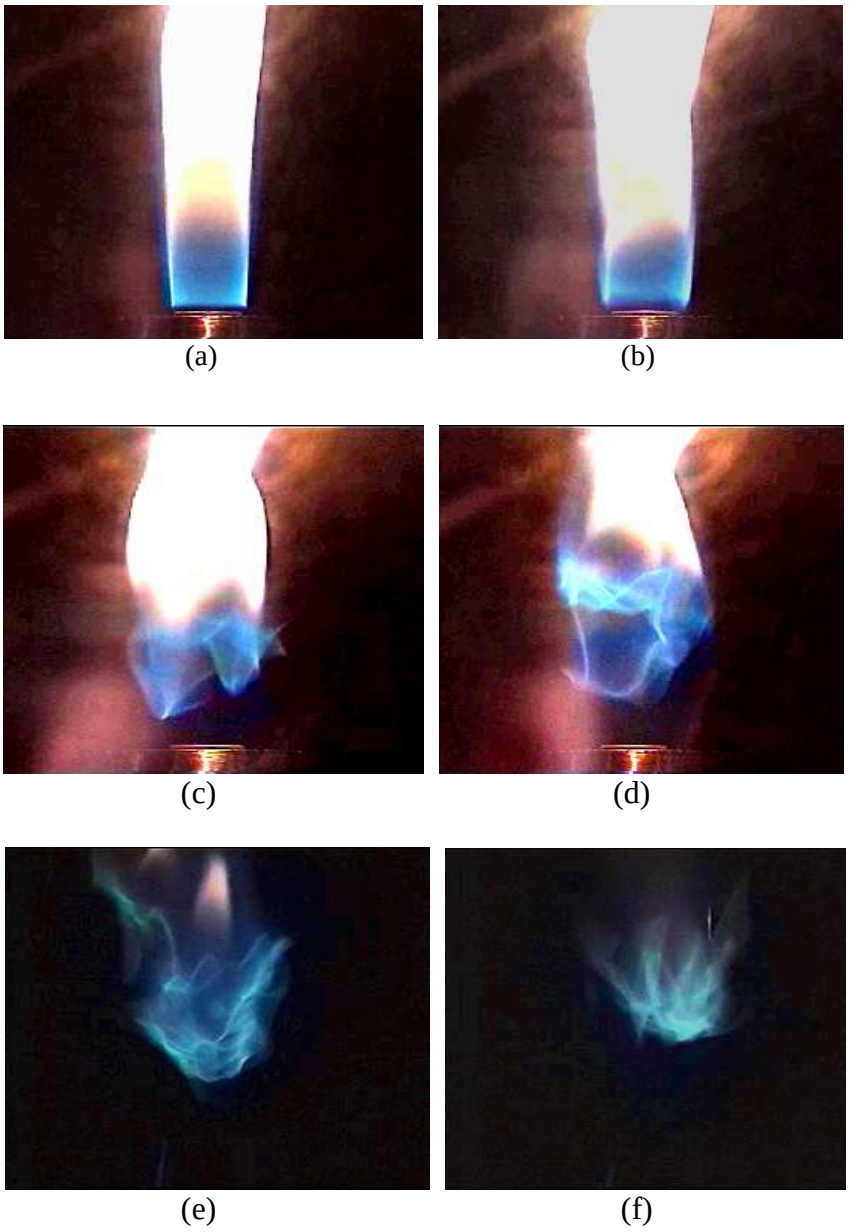

Figure 4.10: Propane velocity constant at propane velocity of 6.3 cm/s.

No rotation, (a) $V_{aa} = 0$, (b) $V_{aa} = 35.5$ cm/s

With rotation, $\omega = 2760$ rpm

(c) $V_{aa} = 46.2$ cm/s, (d) $V_{aa} = 63.9$ cm/s,

(e) $V_{aa} = 92.4$ cm/s, (f) $V_{aa} = 106.6$ cm/s.

A schematic of the fuel flow pattern subject to an annular air, as well as a tube rotation is shown in Figure 4.11.

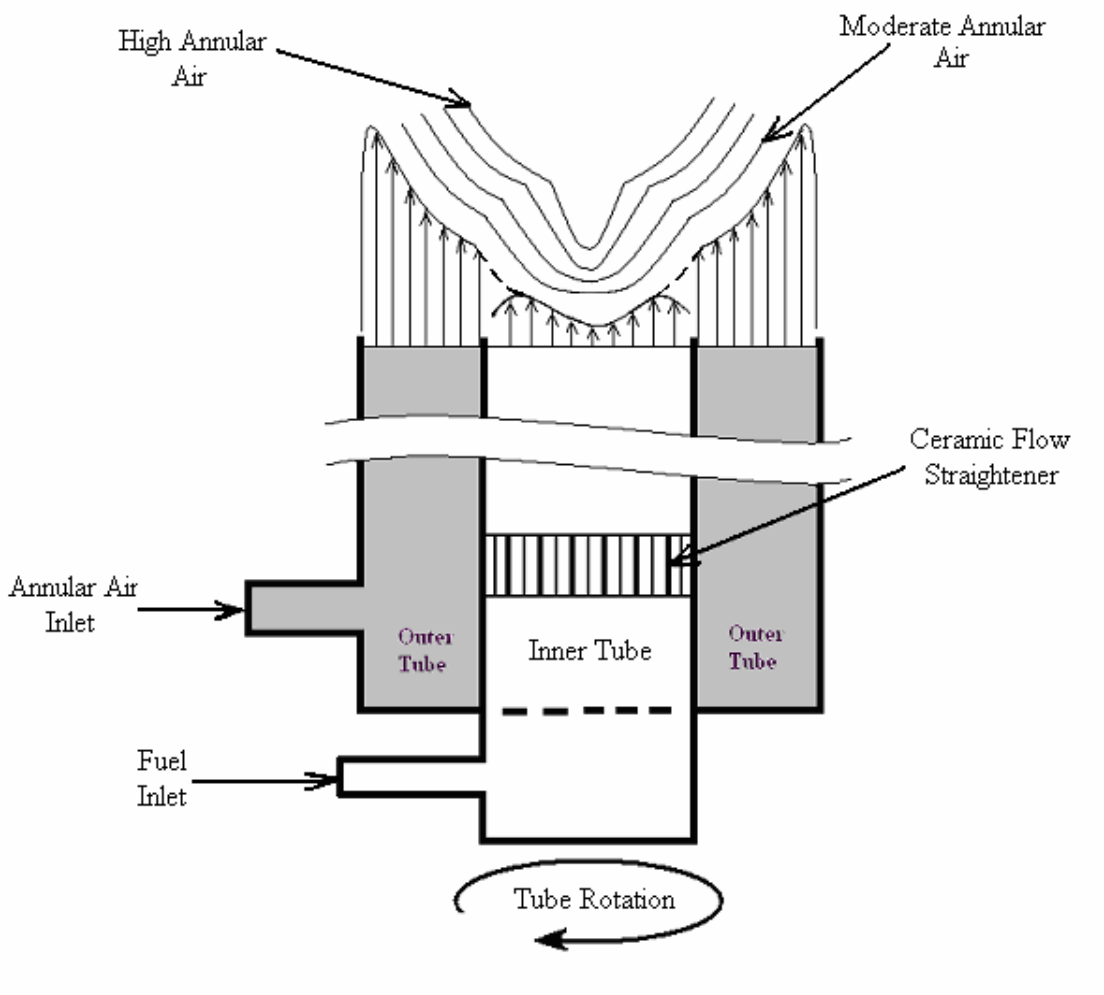

Figure 4.11: The schematic illustration of fuel flow subjected with application of annular air and as well as tube rotation.

4.4 Nonpremixed flame height

4.4.1 No annular air

Figure 4.12 shows the effect of rotation on the nonpremixed flame height from a circular nozzle burner. The fuel velocity increases from 3.4 cm/s to 22 cm/s. These velocities correspond to Re of 53 and 322, which is laminar in nature. For the nonrotating case the flame height increases with a drastic increment in real low flow region and then increases quite steadily for the rest of the flow velocity. To see the effect of rotation on flame height, the burner is rotated at two different speeds: 2190 and 3240 rpm. As shown in Figure 4.12, burner rotation causes the flame height at every fuel velocity to decrease and in some cases, (ω = 3240 rpm, V = 21 cm/s) the flame height reduction goes to 7.6-burner diameters (or 2.85 in). Burner rotation causes the gaseous fuel to have better mixing with ambient air. This causes the flame speed to increase and hence moves the flame upstream that is toward the direction of the burner port. Therefore, at every fuel velocity, for burner rotating at a speed of 2190 rpm, the flame reduces in height. The general effect of burner rotation for circular nozzle burner, as shown in Figure 4.12 is that, the higher the rotational speed (3240 rpm) the lower the flame height. However, the amount of reduction is not significant for different burner speed.

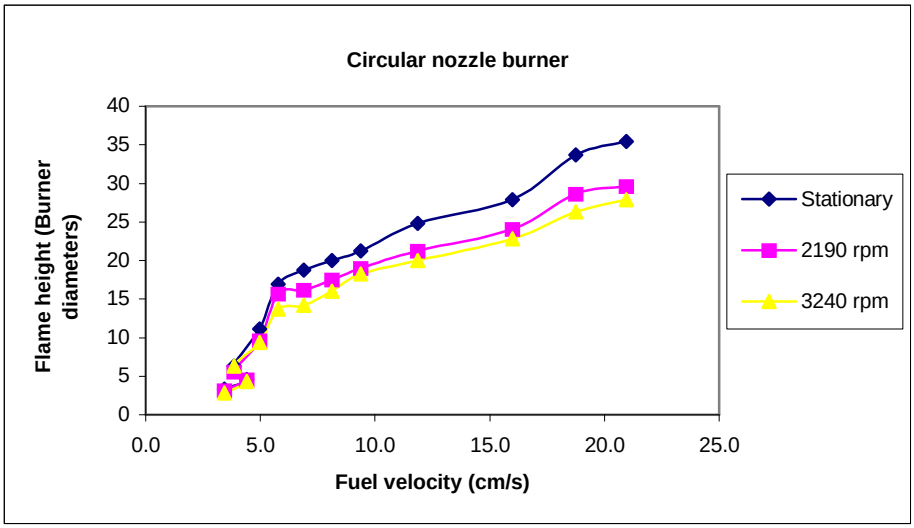

Figure 4.12: Nonpremixed flame height for circular nozzle burner at several burner rotational speed.

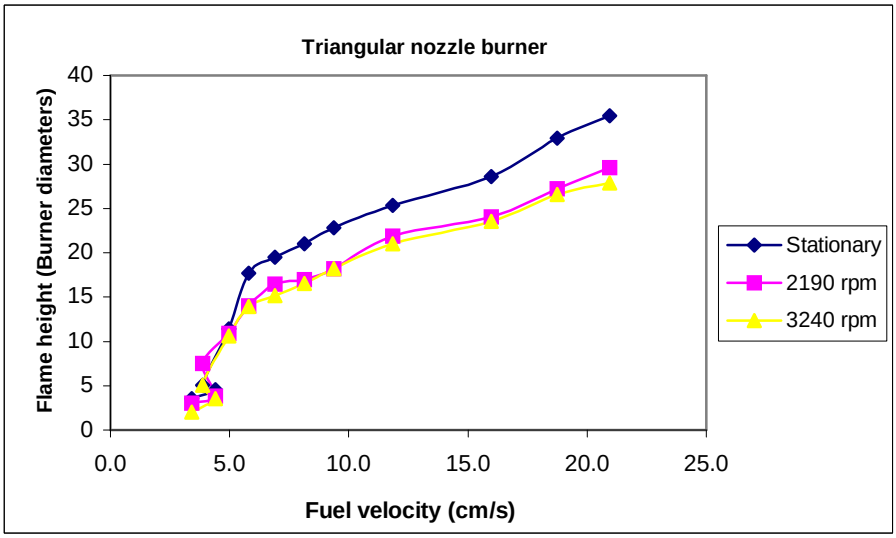

Figure 4.13: Nonpremixed flame height for triangular nozzle burner at several burner

rotational speeds.

Figure 4.13 shows the effect of a triangular nozzle on the flame height. A similar pattern for the flame height for circular nozzle is observed. Rotation of 2190 rpm causes the flame to reduce in height. Further increase in the rotational speed (to 3240 rpm) does much less height reduction compared to the one circular nozzle. The height reduction is also observed by increasing the burner rotational speed but this time the reduction of height is pretty much follows the burner speed.

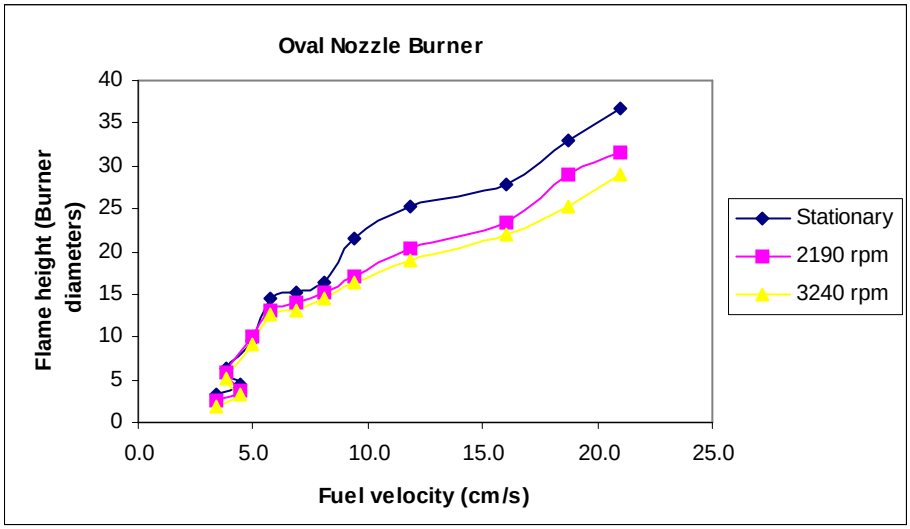

Figure 4.14: Nonpremixed flame height for oval nozzle burner at several burner rotational speeds.

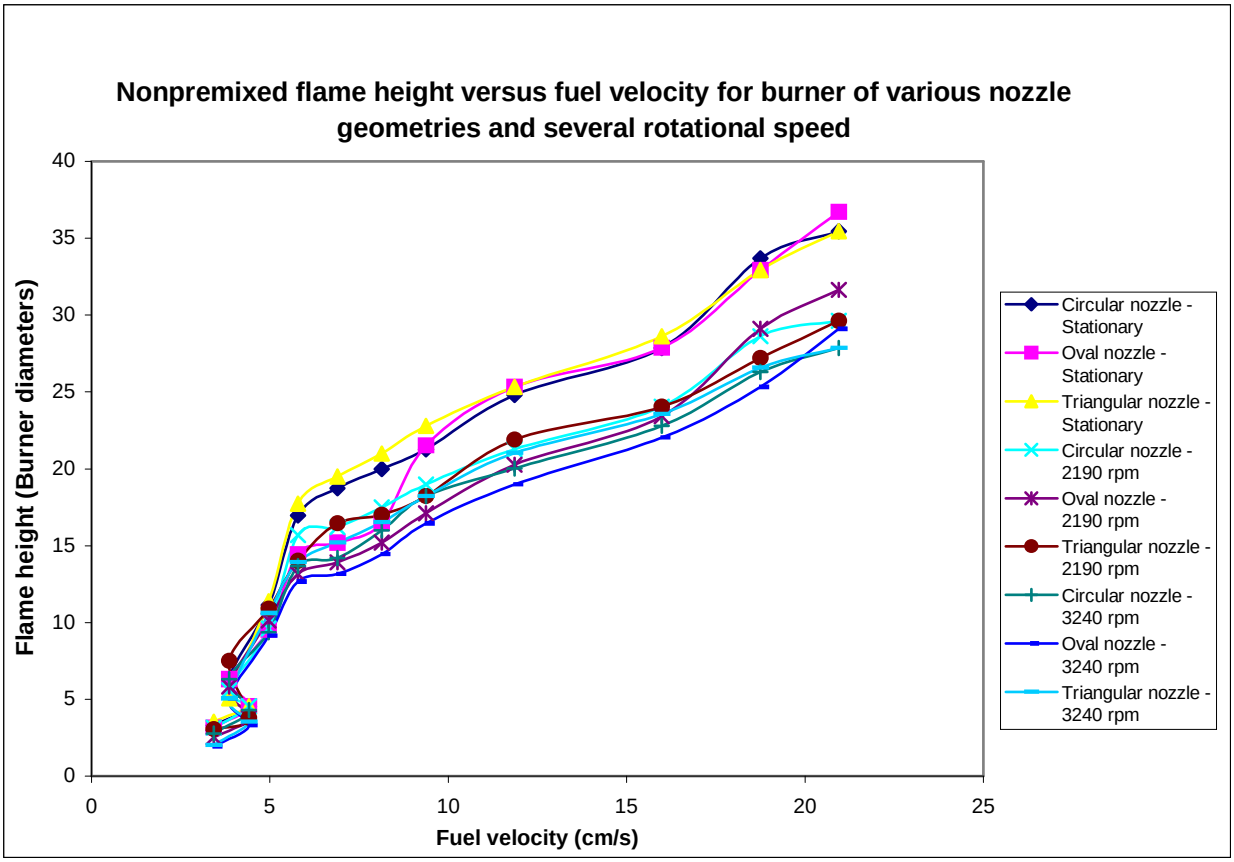

Figure 4.15: Flame height versus fuel velocity for burner of various nozzle geometries and several burner rotational speeds.

Figure 4.15 shows the full effect of flame height due to changes in nozzle geometry and burner rotation. Various nozzle geometries, such as circular, oval and triangular, are used. Range of fuel velocity is from 3.4 cm/s to 22 cm/s, which correspond to Re of 53 to 322. For the nonrotating case the flame height increases with a drastic increment in real low flow region and then increases quite steadily for the rest of the flow velocity. Similar flame height pattern are shown for burner of oval nozzle as well as the triangular nozzle. This shows that for nonrotating burner having a laminar flow characteristic (Reynolds number up to 322), the nozzle geometry does not really

affect the flame height. A significant change is observed only when the burner is rotating. The degree of flame reduction due to rotation varies according to the nozzle shapes and there is really no stands out nozzle shape that affect the flame height that much. The lowest flame height is attained from the oval nozzle rotating at 3240 rpm.

4.4.2 With annular air

In the following section the effect of annular air on the flame height will be discussed. Starting with circular nozzle burner, Figure 4.16 shows the whole effect of burner rotation with and without the application of annular air on diffusion flame height. As depicted in the figure, the flame height reduces slightly due to the application of 71cm/s (Re = 347) annular air. The second greater reduction in flame height is due to the burner rotation of 2190 rpm, without annular air. The third higher reduction is due to the rotation of 3240 rpm, without annular air. The fourth greater reduction is due to burner rotation of 2190 rpm with the application of annular air. Finally the greatest reduction of flame height is due to burner rotation of 3240 rpm with the application of annular air.

As discussed in premixed flame chapter, rotation reduces the velocity of the central part of the jet flame, thus reducing the flame height. Application of annular air increases the opportunity of mixing between oxidizer and the central fuel jet. Furthermore burner rotation increases the swirling action of annular air thus enhances mixing even more. Mixing is the key factor that controls the reaction in nonpremixed flames. The higher the mixing the greater rich fuel can get diluted and hence increasing 1the flame speed. It is also observed that as the fuel velocity increases the gap between the flame heights widens, causing greater reduction in flame height.

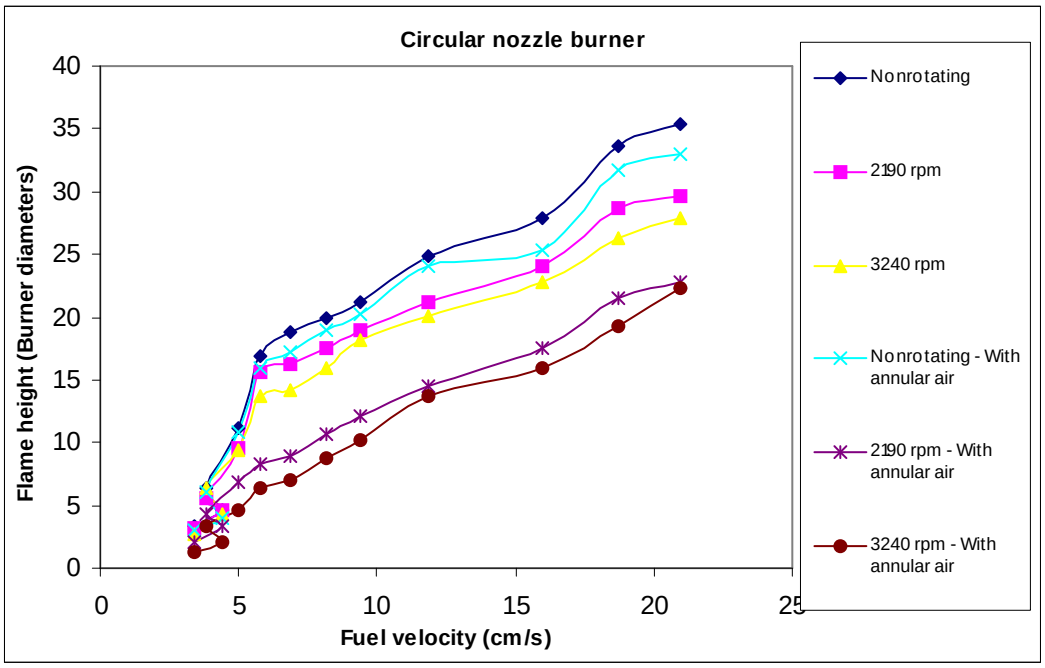

Figure 4.16: The effect of annular air on nonpremixed flame height for circular nozzle burner rotating at several rotational speeds

The effect of annular air on nonrotating and rotating diffusion flame using burner of various nozzle geometries is shown in Figures 4.17 (a) and (b), respectively. For the nonrotating burner shown in Figure 4.17, application of annular air and the use of burner nozzle does not change the flame height significantly. The reduction in flame height is much more obvious by burner rotation and additionally with application of annular air such as shown in Figure 4.17(b). Flowing annular air provides greater opportunity of mixing between oxidizer and the central fuel jet. As a result, the application of 71 cm/s annular air reduces the flame height. The reduction is the most for the oval nozzle.

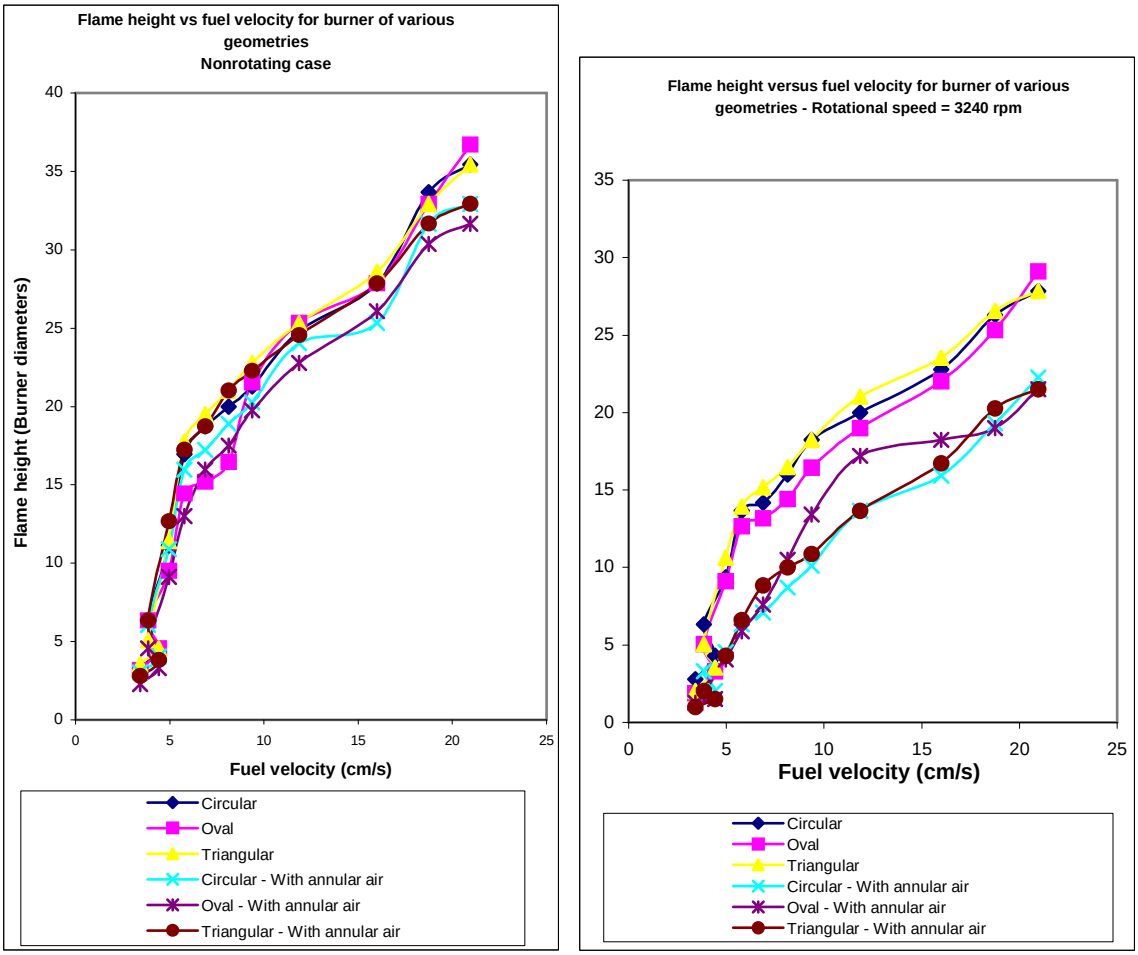

(a) *(b)*

Figure 4.17: Flame height versus fuel velocity for burner of various nozzle geometries, with and without rotation.
(a) Nonrotating, (b) Rotating at 3240 rpm

Chapter 5

SUMMARY AND CONCLUDING REMARKS

In this study, the characteristics of premixed and nonpremixed flames of propane in rotating concentric burner have been experimentally investigated.

Lean premixed-flame investigation is categorized into three parts: low, moderate and high velocity jets. In the low jet velocities, as the burner tube starts to rotate, the flame shape is dramatically altered. The outer flame cone is shown to become wider and shorter in height. The rotating premixed flame is buckled forming a cusp flame shape. For moderate jet flow velocities (around 100 cm/s), burner rotation causes the flame to show a set of double cons, with one higher than the other. When the burner rotation is doubled the flame also shows double appearance. For very lean mixtures (ϕ = 0.22) flowing at moderate velocities (100 cm/s), increasing burner rotational speed to 2760 rpm causes the flame to immerse into the burner tube. The flame completely disappears into its burner port at high rotational speeds, such as 4500 rpm. For mixtures flowing at moderate velocity but with higher equivalence ratio (ϕ = 0.89), burner rotation of 3240 rpm causes the flame to become unsteady and wiggle around the burner rim.

The characteristics of the lean flames with high flow velocities (e.g. 275 cm/s) are quite different. A tall flame does not buckle as the burner rotates, but shows a very dynamic appearance. The flame rotates and shakes vigorously on the burner rim. The effect of rotation on the stabilization of propane-air premixed flames was also

experimentally investigated. In particular, the flame shape is controlled by variation of the axial velocity of the jet, as well as their angular velocities.

An extensive experiment on the low velocity nonpremixed flames have also been conducted. Small-nonpremixed flames exhibit easier mixing in rotating burner. However in transient study of nonpremixed flame, burner rotation in the beginning results in the formation of a soot wings on top of the flame cone. But as the rotation established, the orange region in the flame decreases and a bright blue flame, indicating complete mixing between fuel and air, replaces it. So rotation in this regard helps in mixing and thus enhances combustion.

References

[1] J.H. Grover, M.G. Kessler, and A.C. Scurlock. *Jet Propul.* 30:386-391, 1957.

[2] N.A. Chigier, and A. Chervinsky. *Eleventh Symposium (International) on Combustion*. The Combustion Institute, Pittsburgh, pp. 489-499, 1967.

[3] D.G. Liley. *AIAA J*. 15:1063-1078, 1977.

[4] M.J. Oven, F.C. Gouldin, and W.J. McLean. *Seventeenth Symposium (International) on Combustion.* The Combustion Institute, Pittsburgh, pp. 363-374, 1979.

[5] J.M. Cha, and S.H. Sohrab. *Combustion and Flame*, 106:467-477, 1996.

[6] W.J. Sheu, and S.H. Sohrab, G.I. Sivashinski. *Combustion and Flame*, 79:190-198, 1990.

[7] D.F. Bidinger, and S.H. Sohrab, 1985, unpublished.

[8] Z.H. Chen, G.E. Liu, and S.H. Sohrab. *Combust. Sci. Technol.*, 51:39-50, 1987.

[9] T.H. Lin, and S.H. Sohrab. *Combust. Sci. Technol*., 52:73-79, 1987.

[10] G.I. Sivashinski, and S.H. Sohrab. *Combust. Sci. Technol.*, 53:67-74, 1987.

[11] G.I. Sivashinski, Z. Rakib, M. Matalon, and S.H. Sohrab. *Combust. Sci. Technol.*, 57:37-53, 1988.

[12] T. Kawamura, K. Asato, and T. Mazaki. *Combust. Sci. Technol*., 22:211-216, 1980.

[13] S.H. Sohrab and C.K. Law. *Combustion and Flame*, 62:243-254, 1985.

[14] A.K. Gupta, D.G. Liley, and N. Syred. *Swirl Flows*, Abacus Press, Ohio, 1984.

[15] J.M. Beer, and N.A. Chigier. *Combustion Aerodynamics*, Applied Science Publishers, Florida, 1983.

[16] J.M. Beer, N.A. Chigier, and K.B. Lee. *Ninth Symposium (International) on Combustion*, The Combustion Institute, Pittsburgh, pp. 892-900, 1963.

[17] A.K. Gupta, M.J. Lewis, and M. Daurer. Swirl Effects on Combustion Characteristics of Premixed Flames. *Journal of Engineering for Gas Turbine and Power*, Vol. 123, July 2001.

[18] J.M. Cha and S.H. Sohrab. *Combustion and Flame*, 106:467-477, 1996.

[19] R.H. Chen and J.F. Driscoll. *22nd Symposium (Intern.) on Combustion*, The Combustion Institute, Pittsburgh, pp. 531-540, 1988.

[20] T.C. Claypole and N. Syred. *18th Symposium (Intern.) on Combustion*, The Combustion Institute, Pittsburgh, pp. 81-89, 1981.

[21] C.K. Chan and R.K. Cheng. *24th Symposium (Intern.) on Combustion*, The Combustion Institute, Pittsburgh, pp. 511-518, 1992.

[22] R.W. Schefer. Combustion of hydrogen-enriched methane in a lean premixed swirl burner. *Proceeding of the 2001 DOE Hydrogen program Review*, NREL/CP-570-30535, 2001.

[23] T.S. Cheng, Y.-C. Chao, D.-C., Wu, T. Yuan, C.-C. Lu, C.-K. Cheng, J.-M. Chang. *27th Symposium (Intern.) on Combustion*, The Combustion Institute, Pittsburgh, pp. 1229-1237, 1998.

[24] T.C. Claypole, and N. Syred. *18th Symposium (Intern.) on Combustion*, The Combustion Institute, Pittsburgh, PA, pp. 81-89, 1981.

[25] R. Hillemanns, B. Lenze, and W. Leuckel. *21st Symposium (International) on Combustion*, Combustion Institute, pp.1445-1453, 1986.

[26] S. Turn. *Introduction to Combustion*, McGraw Hill, 1996.

[27] J.M. Cha and S.H. Sohrab. *Combustion and Flames,* 106:467-477, 1996.

[28] R.H. Chen and J.F. Driscoll. *23rd Symposium (International) on Combustion*, The Combustion Institute, Pittsburgh, pp. 281-288, 1990.

[29] J.M. Chang. Effects of fuel-air mixing on flame structures and NOx emissions in swirling methane jet flames. *27th Symposium (International) on Combustion*, University of Colorado at Boulder, CO, pp. 2-7, August 1998.

[30] V.J. Lyons. Fuel-air nonuniformity reaction on nitric oxide emissions. *AIAA J.*, 20 (5), 660, 1981.

[31] T.F. Fric. Effects of fuel-air unmixedness on NOx emissions. *J. Propulsion and Power* 9 (5), 708, 1993.

[32] J. Tomeczek, J. Goral, and B. Gradon. Gasdynamic abatement of NOx emission from industrial natural gas jet diffusion flames, *Combust. Sci. and Tech.*, 105, 55-65, 1995.

[33] R. Hillemans, B. Lenze, and W. Leuckel. Flame stabilization and turbulent exchange in strongly swirling natural gas flames. *21st Symposium (International) on Combustion*, The Combustion Institute, Pittsburgh, PA, pp. 1445-1453, 1986.

[34] R.H. Chen and J.F. Driscoll. The role of the recirculation vortex in improving fuel-air mixing within swirling flames. *22nd Symposium (International) on Combustion*, The Combustion Institute, Pittsburgh, pp. 531-54,1988.

[35] R.E. Charles, J.L. Emdee, L.J. Muzio, and G.S. Samuelsen. The effect of inlet conditions on the performance and flowfield structure of a non-premixed swirl-stabilized distributed reaction. *21st Symposium (International) on Combustion*, The Combustion Institute, Pittsburgh, PA, pp. 1455-1461, 1986.

[36] S.H. Starner, and R.W. Bilger. Further velocity measurements in turbulent diffusion flame with moderate swirl, *Combust. Sci. and Tech.,* 63, 257-274, 1989.

[37] D. Shen, J.M. Most, P. Joulain, and J.S. Bachman. The effect of initial conditions for swirl turbulent diffusion flame with a straight-exit burner, *Combust. Sci. and Tech.*, 100, 203-224, 1994.

[38] A. Coghe, and G. Solero. Analisi del miscelamento turbolento aria/combustibile nel modello di un combustore a bassa produzione di NOx, *Final Enea Report*, 1997.

[39] G. Solero, G. Brunello, and A. Coghe. Effects of injection typology on turbulent mixing in the primary region of a homogeneous combustor, *Combustion Meeting '98*, Ravello, pp. 26-28, May 1998.

[40] A.K. Gupta, D.G. Lilley, and N. Syred. *Swirl Flows*, Abacus Press, Turnbridge Wells, UK, 1984.

[41] A.D. Birch, D.R. Brown, M.G. Dodson, and J.R. Thomas. The turbulent concentration field of a methane jet, *J. Fluid Mech.* 88 Part 3, 431, 1978.

[42] E. Villermaux. Mixing and spray formation in coaxial jets, *J. Propulsion and Power*, 14 (5), 807-817, 1998.

[43] Y.C. Chao, J.M. Han, and M.S. Jeng. A quantitative laser sheet image processing method for the study of the coherent structure of a circular jet flow, *Experiments in Fluids* 9, 323-332, 1990.

ii) Contoh format bagi halaman judul (hadapan) bagi laporan Akhir Penyelidikan

Maklumat yang perlu ada :

a) Judul lengkap penyelidikan disertakan judul dalam bahasa kedua dalam kurungan (huruf besar)
b) Nama penuh penyelidik seperti dalam kad pengenalan atau pasport antarabangsa (huruf besar)
c) Vot. No
d) Nama Fakulti/Institut/Pusat/Jabatan tempat penyelidik berdaftar (Awalan abjad pada setiap perkataan adalah besar)
e) Nama Universiti (Awalan abjad pada setiap perkataan adalah besar)
f) Tahun diserahkan

VOT 71049

Judul lengkap penyelidikan

A NEURAL NETWORK APPROACH FOR STOCK MARKET INDEX PREDICTION

(PERAMALAN INDEKS PASARAN SAHAM MENGGUNAKAN PENDEKATAN RANGKAIAN NEURAL)

Nama penuh penyelidik

BAHROM BIN SANUGI
SAN WOON SHANG

RESEARCH VOTE NO:
71049

Nama Fakulti/Institut/ Pusat/Jabatan

Jabatan Matematik
Fakulti Sains
Universiti Teknologi Malaysia

Tahun diserahkan

1996

UNIVERSITI TEKNOLOGI MALAYSIA

BORANG PENGESAHAN
LAPORAN AKHIR PENYELIDIKAN

TAJUK PROJEK : STUDIES ON THE EFFECT OF SWIRL INTENSITY AND FUEL MIXTURES ON COMBUSTION AND FLAME CHARACTERISTICS OF SWIRL BURNER

Saya MAZLAN ABDUL WAHID
(HURUF BESAR)

Mengaku membenarkan **Laporan Akhir Penyelidikan** ini disimpan di Perpustakaan Universiti Teknologi Malaysia dengan syarat-syarat kegunaan seperti berikut :

1. Laporan Akhir Penyelidikan ini adalah hakmilik Universiti Teknologi Malaysia.
2. Perpustakaan Universiti Teknologi Malaysia dibenarkan membuat salinan untuk tujuan rujukan sahaja.
3. Perpustakaan dibenarkan membuat penjualan salinan Laporan Akhir Penyelidikan ini bagi kategori TIDAK TERHAD.
4. * Sila tandakan (/)

☐	SULIT	(Mengandungi maklumat yang berdarjah keselamatan atau Kepentingan Malaysia seperti yang termaktub di dalam AKTA RAHSIA RASMI 1972).
☐	TERHAD	(Mengandungi maklumat TERHAD yang telah ditentukan oleh Organisasi/badan di mana penyelidikan dijalankan).
☑	TIDAK TERHAD	

TANDATANGAN KETUA PENYELIDIK

Mazlan Abdul Wahid
Nama & Cop Ketua Penyelidik

Tarikh :

CATATAN : ***** *Jika Laporan Akhir Penyelidikan ini SULIT atau TERHAD, sila lampirkan surat daripada pihak berkuasa/organisasi berkenaan dengan menyatakan sekali sebab dan tempoh laporan ini perlu dikelaskan sebagai SULIT dan TERHAD.*